Title

The Implications of Brain-Derived Neurotrophic Factor in the Biological Activities of Platelet-Rich Plasma

Journal

Inflammation, 48(1)

ISSN

0360-3997

Authors

Malange, Kaue Franco

de Souza, Douglas Menezes

Lemes, Julia Borges Paes

et al.

Publication Date

2025-02-01

DOI

10.1007/s10753-024-02072-9

Inflammation (2025) 48:426–446
https://doi.org/10.1007/s10753-024-02072-9

RESEARCH

The Implications of Brain-Derived Neurotrophic Factor in the Biological Activities of Platelet-Rich Plasma

Kaue Franco Malange[1] · Douglas Menezes de Souza[2,3] · Julia Borges Paes Lemes[1] · Cecilia Costa Fagundes[1] · Anna Lethicia Lima Oliveira[1] · Marco Oreste Pagliusi[1] · Nathalia Santos Carvalho[1] · Catarine Massucato Nishijima[1] · Cintia Rizoli Ruiz da Silva[3] · Silvio Roberto Consonni[3] · Cesar Renato Sartori[1] · Claudia Herrera Tambeli[1] · Carlos Amilcar Parada[1]

Received: 24 March 2024 / Revised: 16 May 2024 / Accepted: 31 May 2024 / Published online: 21 June 2024

Abstract

Platelet-rich plasma (PRP) is a biological blood-derived therapeutic obtained from whole blood that contains higher levels of platelets. PRP has been primarily used to mitigate joint degeneration and chronic pain in osteoarthritis (OA). This clinical applicability is based mechanistically on the release of several proteins by platelets that can restore joint homeostasis. Platelets are the primary source of brain-derived neurotrophic factor (BDNF) outside the central nervous system. Interestingly, BDNF and PRP share key biological activities with clinical applicability for OA management, such as anti-inflammatory, anti-apoptotic, and antioxidant. However, the role of BDNF in PRP therapeutic activities is still unknown. Thus, this work aimed to investigate the implications of BDNF in therapeutic outcomes provided by PRP therapy *in vitro* and *in-vivo*, using the MIA-OA animal model in male Wistar rats. Initially, the PRP was characterized, obtaining a leukocyte-poor-platelet-rich plasma (LP-PRP). Our assays indicated that platelets activated by Calcium release BDNF, and suppression of M1 macrophage polarization induced by LP-PRP depends on BDNF full-length receptor, Tropomyosin Kinase-B (TrkB). OA animals were given LP-PRP intra-articular and showed functional recovery in gait, joint pain, inflammation, and tissue damage caused by MIA. Immunohistochemistry for activating transcriptional factor-3 (ATF-3) on L4/L5 dorsal root ganglia showed the LP-PRP decreased the nerve injury induced by MIA. All these LP-PRP therapeutic activities were reversed in the presence of TrkB receptor antagonist. Our results suggest that the therapeutic effects of LP-PRP in alleviating OA symptoms in rats depend on BDNF/TrkB activity.

KEY WORDS BDNF · PRP · platelets · osteoarthritis · inflammation · joint pain

Introduction

Degenerative joint diseases are currently one of the biggest causes of physical disability worldwide, and osteoarthritis (OA) is one of the primary sources [1–3]. This disease is commonly linked with a gradual increment in oxidative stress and insufficient repair mechanisms inside the joint space, which is typically seen as an aging outcome [3–5]. Genetics, lifestyle, and imbalance in bone remodeling are other potential triggers of OA [3–5].

Chronic pain is still the primary symptom of OA, resulting from a lack of effective therapies to mitigate joint inflammation and diminish disease remission [4, 6]. In such a context, platelet-rich plasma therapy (PRP) has emerged as a potential therapeutic approach for OA management [7]. The mechanism in which PRP induces repair in arthritic joints is

✉ Carlos Amilcar Parada
caparada@unicamp.br

1 Department of Structural and Functional Biology, Institute of Biology, University of Campinas (UNICAMP), Rua Carl Von Linnaeus, Cidade Universitária Zeferino Vaz, Campinas, São Paulo 13083-864, Brazil

2 Department of Pharmacology, School of Medical Sciences, University of Campinas (UNICAMP), Rua Tessália Vieira de Camargo, 126, Cidade Universitária Zeferino Vaz, Campinas, São Paulo 13083-887, Brazil

3 Department of Biochemistry and Tissue Biology, Institute of Biology, University of Campinas (UNICAMP), Rua Monteiro Lobato, 255, Cidade Universitária Zeferino Vaz, Campinas, São Paulo CEP 13083-862, Brazil

linked with the release of several growth factors by platelets capable of triggering tissue anabolism, macrophage polarization, and angiogenesis [7, 8]. Altogether, these biological activities allow the switch in the inflammatory and degenerative state at the intra-articular space, providing a better disease outcome for OA patients [9, 10].

Although platelets have a versatile collection of growth factors stored in their cytosolic granules [7], they serve as primary sources of Brain-Derived growth factor (BDNF) at the periphery, carrying significantly higher amounts of this protein in comparison with brain extracts [11–13].

BDNF was discovered in 1982 [14], being reported as a protein present in the mammalian brain capable of inducing survival and neurite outgrowth in neurons [15]. Outside of the nervous system, studies have shown anti-inflammatory, antiapoptotic activities of this neurotrophin at the periphery [14, 16–20]. These same therapeutic activities are also seen for PRP [7, 21, 22]. However, it is still unknown if BDNF plays a significant role in platelet repair mechanisms, especially those provided with PRP therapy in OA joints.

Thus, the study aimed to investigate the role of BDNF in therapeutic activities induced by PRP *in vitro*, and in vivo, using the monoiodine acetate (MIA) model of osteoarthritis in rats [1–4, 6, 7, 7, 11–14, 16–36].

Materials and Methods

Animals

Male Wistar rats (200-220 g) were acquired from the Central Animal Facility of the University of Campinas (CEMIB, UNICAMP) and kept in polypropylene cages in the maintenance vivarium from the Pain Studies Lab—UNICAMP at a temperature of 22 ± 2 °C, with a 12-h light/dark cycle with food and water ad libitum. All animal experiments were approved by the Animal Use Ethics Committee from the Institute of Biology at UNICAMP, protocols 4706-1 and 4834-1A. All behavioral experiments followed the guidelines recommended by the International Association for the Study of Pain – IASP for the assessment of animal behavior in research animals [37].

PRP Obtainment and Characterization

To obtain an appropriate amount of PRP for experiments, 18 animals served as blood donors. The samples were characterized and quantified at each centrifugation step. The plasma samples were then mixed to create a pool for *in-vitro*/*in-vivo* experiments and were subjected to hematology quantification. The terminology used to describe the samples was assessed following the MARSPILL guidelines [38].

PRP preparation was carried out following the Amable et al. (2013) protocol [39] with some modifications. Initially, animals were terminally anesthetized with Ketamine (300 mg/kg; 200 µL) and Xylazine (30 mg/kg;200 µL) co-injected intraperitoneally. A thoracotomy was performed for the retrieval of 5 mL of blood from each animal through a vein puncture of the hepatic vena cava. The blood collected was sent to sterile tubes containing citric acid dextrose anticoagulant solution (Vacutainer BD™). After, an amount of 0.5 ml of blood samples from each donor (Whole blood) was separated and the remaining 3.5 ml aliquot was destined to sterile silicone tubes (Labor Import™) for centrifugation (300G; 18 °C; 5 min). In sequence, 500 µL of the platelet-rich plasma disposed on the upper layer of the tube was collected and sent to a hematology counter (Micro ES60; Horiba™). After this step, the samples were subjected to a second centrifugation (700G; 18 °C; 17 min). Then, the upper-half plasma which comprehends the poor-platelet-plasma (PPP) was collected and the remaining volume, which consists of pure-platelet-rich plasma (P-PRP), or leukocyte-poor-platelet-rich plasma (LP-PRP) was homogenized and further collected. The P-PRP/LP-PRP samples were submitted to the hematology counter being PPP used as control.

Platelet Degranulation Assay and Measurement of BDNF Release

To investigate the BDNF release by platelets, an assay was carried out with LP-PRP samples stimulated with 10% Calcium Chloride (10%; CaCl2; agonist of platelet degranulation) [28, 40]. Initially, an amount of 1 mL from both LP-PRP and PPP samples was previously obtained and filtered on a 0.22 µm filter. Then, 160 µL/well of sterile LP-PRP or PPP was pipeted on 5 wells from a 48-well cell-culture plate. In sequence, 40 µL of 10% $CaCl_2$ solution was added to each well, and samples were left for 60 min in a flow cabinet at 22 ± 2 °C room temperature. After the clott gel formation, the samples were resuspended in 450 µL of sterile PBS solution for growth factors retrieval and were left for 30 min in an incubator at 37 °C/5%CO_2. Then, samples were collected and centrifuged (8500 rpm; 15 min; 4 °C). The supernatant was collected for a quantitative analysis of the BDNF released in LP-PRP and PPP samples through ELISA assay, according to the manufacturer's instructions (R&D system™; DY248). Following the same procedures, experiments with LP-PRP and PPP samples without activation were carried out together as a control.

Another aliquot of the supernatant collected was filtered through a 0.22 µM filter and later destined for the macrophage polarization assay. In an extra-set experiment and supplementary control, the clot gel formed on the cell plate was imaged using the bright field of a fluorescence

microscope (Leica, DMI 6000B, Leica Microsystems, Germany) for the detection of the fibrin network, another resulting phenome from platelet activation [41].

Cell Culture of Bone Marrow-Derived Macrophages

Bone marrow-derived macrophages (BMDMs) were obtained following the protocol described by Toda et al. (2021) [42]. Initially, bone marrow hematopoietic stem cells from femur and tibia of *Wistar* rats were collected and plated (1×10^4 cells/well) in 24-well plates containing RPMI medium (R6504; Sigma aldrich™) supplemented with 10% fetal bovine serum (12103C; Sigma aldrich™), 1% penicillin–streptomycin (P4333; Sigma aldrich™), 1% non-essential amino acid solution (M7145; Sigma aldrich™), 1% solution of vitamins (M6895; Sigma aldrich™), 1% sodium pyruvate (P2256; Sigma aldrich™) and 20 ng/mL macrophage colony-stimulating factor (M-CSF; Z03010-5; Genscript™). The cell medium was changed on the 3rd day after the initial plating and on the fifth day, the culture medium was changed and added with different treatments intended for the polarization assay.

Macrophage Polarization and SLPPRP Treatment Assay

Carried out with BMDMs previously obtained, macrophage cells were polarized to the M1 profile. All drugs were dissolved in a cell culture medium according to the experimental group assigned.

First, five groups were adopted following the experimental design below: three groups, the M1 (LPS/IFN-γ), M1 plus an antagonist of TrkB receptor (LPS/IFN-γ/ANA-12), and M1 plus vehicle (LPS/IFN-γ/Vehicle), were stimulated with 300 µL of cell culture medium containing LPS (20 ng/mL; Sigma Aldrich™) and IFN-γ (20 ng/mL; Invitrogen™) added with, respectively, ANA-12 (100 µM; Alomone Lab™) or its vehicle (1% DMSO; Sigma Aldrich™). Then, 60 min after stimuli, these groups were treated with 150 µL of culture medium. The other two groups, LPS/IFN-γ/ANA-12 + LP-PRP and LPS/IFN-γ/SLPPRP consisted respectively of BMDM cells stimulated with 300 µL of cell culture medium containing LPS/IFN-y/ANA-12 or LPS/IFN-y only, at the same concentrations mentioned above, and 60 min after treated with 150 µL of the supernatant collected on platelet activation assay (SLPPRP). At 180 min after LPS/IFN-γ, all groups were submitted to cell lysate for RNA extraction.

As supplemental controls, the following groups were adopted: control, ANA-12, and Vehicle. These groups consisted respectively of BMDM cells cultured initially in 300 µL medium or 300 µL with medium containing ANA-12 (100 µM) or its vehicle (1% DMSO). Then, after 60 min, these groups received more than 150 µL of culture medium and were also sent to cell lysate and RNA extraction in 180 min after the first treatment.

The M1 and M2 macrophage phenotypes were assessed, respectively, through the gene expression of *Nos-2* and *Arg-1* by quantitative real-time PCR (RT-qPCR).

RNA Extraction and Quantitative Real-Time PCR Analysis (RT-qPCR)

RNA extraction was performed using Trizol reagent and RNA extraction kit (Tri-Reagent, T9424; Sigma-Aldrich®), following the manufacturer's instructions. Complementary DNA (cDNA) synthesis was performed using the Accuris qMax kit (Accuris, Benchmark Scientific, New Jersey, USA) following the manufacturer's instructions. The gene expression of *Nos-2* and *Arg-1* genes (see Table 1 for primer sequences) was determined by real-time PCR performed in a StepOnePlus system (Applied Biosystems™, USA) using the iTaq Universal SYBR Green Supermix reagent (Bio-rad laboratories™, USA). β-actin was used as a housekeeping gene. The relative change in gene expression was calculated using the $2^{-\Delta\Delta Ct}$ method [43].

Intra-Articular Injection

For intra-articular drug administration, the animals were initially anesthetized with isoflurane (Isoforine, Cristália™; 5% for anesthesia induction and 2% for maintenance). After, the tibiofemoral joint was shaved, and asepsis was performed with 70% alcohol solution and 1% povidone-iodine solution (Riodeine; Rioquímica™). Subsequently, the intra-articular injection was performed by flexing the right joint at 45° followed by the introduction through the patellar tendon of a 26G needle (13 × 0.45 mm; BD™) coupled to a Hamilton syringe (Hamilton Company™). For each injection, the total volume injected did not exceed 25 µL.

Table 1 Primer Sequences used for RT-qPCR

Target Gene	Forward sequence 5'-3'	Reverse sequence – 5'-3'
β-actin	CGCGAGTACAACCTTCTTGC	CGTCATCCATGGCGAACTGG
Arg-1	CCAGTATTCACCCCGGCTAC	GTCCTGAAAGTAGCCCTGTCT
Nos-2	TCAGGCTTGGGTCTTGTTAGC	GAAGAGAAACTTCCAGGGGCA

LP-PRP Treatment in Experimental Osteoarthritis and Investigation from the Role of TrkB Receptor

For *in-vivo* investigation of the role of TrkB receptor and the effects induced by LP-PRP treatment, the animals were initially submitted to the experimental osteoarthritis (EOA) induction through an injection on day 0 of monoiodine acetate (MIA group; 2 mg; Sigma Aldrich™) via intra-articular on the tibiofemoral joint from the right knee. The control group consisted of animals injected with NaCl 0.9% solution (Saline group). On day 7, after OA induction, animals were randomly distributed in 4 groups: the leucocyte-poor-platelet-rich plasma group (LP-PRP group) received initially saline solution and 30 min after LP-PRP; the ANA-12 + LP-PRP group, which consisted of animals initially treated with ANA-12 (TrkB receptor antagonist; 100 µM; Alomone Labs™) and 30 min after received LP-PRP; The ANA-12 and ANA-12 Vehicle groups, designed as controls and which consisted of animals respectively treated with a single injection of ANA-12 (100 µM; Alomone Labs™) or its vehicle (1% DMSO; Sigma Aldrich™). This treatment approach was also performed on day 14 after OA induction. The same LP-PRP pool was used for injection in LP-PRP and ANA-12 + LP-PRP groups in all experiments conducted. Behavioral tests were performed on days 0, 3, 7, 14, and 21 post-MIA injections. An adapted electronic von Frey apparatus was used to assess the joint flexion mechanical threshold and the Catwalk System (NoldusTM) evaluated the dynamic motor function of animals on a walking track test. On day 21, animals were euthanized and harvested for the knee joint and L4/L5 dorsal root ganglia (DRG).

Assessment of Mechanical Threshold for Joint Flexion – Adapted Von Frey

The mechanical threshold for knee joint flexion was performed following the methodology of Guerrero et al. (2006) [44] with some modifications. Initially, the animals were placed in acrylic cages (23 × 20x18cm) 60 min before the tests for acclimatization in a quiet room. The cages were attached to a wire grid floor arranged on a suspended platform where at the bottom there is a mirror that allows the proper visualization of the animals during the test. The equipment used was an electronic von Frey (digital analgesimeter; Insight®, Brazil) that consists of a force transducer where at the end a 4.15 mm^2 polypropylene tip is fixed and connected to a device that reads the force applied to the animal paw, converting it to grams. A stimulus is applied to the metatarsal footpad, perpendicularly and in ascending motion until the induction of tibiofemoral joint flexion followed by paw withdrawal. The force required to induce the joint flexion followed by the paw withdrawal reflex is recorded in grams and assumed to be the mechanical threshold to induce such joint flexion. For all experiments, baseline, and post-treatment measurements were performed. The assessment was during the 0 (baseline), 3-, 7-, 14-, and 21-days post-MIA injection. The result represents the arithmetic mean of the 6 measurements performed at each time analyzed.

Assessment of Joint Dynamic Motor Function – Catwalk Walk-Track Test

The assessment of motor function in treated animals was performed using the CatWalk walking track test (Noldus Inc., Wageningen, Netherlands). The equipment consists of an automated system comprehended by a hall coupled with an illuminated walkway glass floor that allows the spontaneous movement of the animal. The green LED plus a red-illuminated background creates a contrast in the glass floor that can be recorded by a high-speed video camera (Gevicam GP-3360; GEViCAM Inc., Milpitas, CA, USA) equipped with a wide-angle lens (6.0 mm; DF6HA-1B, Fujinon Corp., China). The camera is set at 56 cm underneath the walkway. As animals cross a calibrated 20 × 10 cm length lane, paw prints are automatically recorded by the CatWalkTM XT 10.6 software, and the measurement of static and dynamic parameters associated with the animal's gait can be assessed. The gait analysis was performed at 0, 7, 14, and 21 days, after OA induction, always in the afternoon with the room lights switched off. During each period of analysis, each rat performed three runs following the parameters shown in Table 2.

Euthanasia and Tissue Harvest

At the end of experiments on day 21, the animals were terminally anesthetized with Ketamine (300 mg/kg; 200 µL) and Xylazine (30 mg/kg;200 µL), co-injected intraperitoneally and perfused through the ascending aorta with saline followed by a cold 4% paraformaldehyde (PFA) solution containing 0.1 M phosphate buffer. After the perfusion, the right knee joint and L4/L5 DRGs were collected.

Table 2 Catwalk XT Configurations; a.u = Arbitrary Units

Green Intensity 0.35 (a.u)	Max. allowed speed variation 60%	Min & Max crossing time 0.5–8.0 s
Red Ceiling Light 17.8 (a.u)	Green walkaway light 16.5 (a.u)	Camera gain 25.01 (a.u)

Histopathological Analysis of the Tibiofemoral Joint

The collected knee joints were left in a 4% PFA solution for 24 h. After, they were transferred to another container with a decalcifying acid solution (4.5% HCl, EDTA, and Sodium Tartrate). This solution was replaced once per week. On the 14th day, the joints were immersed in paraffin. The joint tissue was sectioned in 5 µm and stained with Hematoxylin/Eosin. For the assessment of quantitative scores in each group analyzed, the histopathological analysis was performed using an optical microscope (Nikon™; E800 model) and following the guidelines of the Osteoarthritis Research Society (OARSI) [45].

Assessment of Neuronal Injury by Quantifying Transcriptional Activating Factor-3 (ATF-3) Staining in Dorsal Root Ganglia Neurons

The harvested DRGs were left for 48 h in a cryoprotectant solution containing 30% sucrose. Then, each DRG was embedded in an OCT compound (Tissuetech, Sakura Finetek, Torrance, CA, USA). Non-serial sections from L4 and L5 DRGs were made at 15 µm and optimum temperature using a cryostat. At least 8 sections were mounted on each slide, being stored at − 20 °C until further fluorescence staining.

For the immunofluorescence detection of ATF-3 in DRG neurons, slides were incubated for 30 min in phosphate buffer saline (PBS) containing 0.1 M glycine and subsequently blocked with 2% of bovine serum albumin (BSA) and triton X-100 0.1% for 1 h. After washing with 0.1 M PBS, the slides were incubated overnight with anti-ATF-3 (1:200, polyclonal rabbit; sc-188, Santa Cruz®) and anti-fox3-protein (NeuN; neuronal marker; 1:1000; mouse monoclonal; Ab104224; Abcam™) primary antibodies in a PBS solution containing 0.1% triton X-100 and 2% BSA. Then, the slides were washed once with the same solution used for the primary antibody and then washed 3 times for 5 min with 0.1 M PBS. In sequence, the sections were incubated with Alexa 594 secondary antibody (donkey; anti-rabbit;1:1000; Life Technologies™) and Alexa 488 (donkey; anti-mouse; 1:1000; Life Technologies™) for 90 min and after were washed 4 times for 5 min in 0.1 M PBS. Then, the slides were incubated for 10 min with DAPI for cell nuclei staining (0.25 µg/mL; Sigma Aldrich™). Negative controls were mounted and consisted of slides incubated only with secondary antibodies to confirm nonspecific binding. The slides were photographed on a confocal microscope (Zeiss™; LSM-780 NLO model) at 20 × magnification.

For the assessment of ATF-3 expression on DRG neurons, three animals per group were adopted and one slide for each animal was analyzed. In the end, an average of 1000 cells and 24 sections per group were analyzed. In each section, the relative percentage expression of ATF-3 on each field analyzed was initially calculated by the formula: the number of neurons labeled with ATF-3 divided by the number of neurons per field × 100. Then, to obtain the normalized arithmetic mean of ATF-3 expression in each section counted, the percentages from each field were summed and further divided by the total number of fields analyzed. The final average obtained corresponds to the data included for the statistical analysis and graphical representation.

Statistical Analysis

The analysis of the results was performed using GraphPad Prism v.8 software (GraphPad™, San Diego, USA). The t-student test was selected when two means were compared. When the comparison involved more than two means, a one-way or two-way analysis of variance (ANOVA) was performed according to the experimental design followed. When the level of significance indicated a statistical difference between the analyzed means, the Tukey test was used to compare the different analyzed groups. The level of significance adopted in the analysis of the results was $p < 0.05$.

Results

Characterization of Platelet-Rich Plasma Samples

Two sequential centrifugations of the whole blood collected were performed to isolate the PRP followed by cell quantification in the hematology analyzer. The results show the characterization from PRP samples of three donors that were sampled for statistical analysis and representation.

As seen in Supplementary Fig. 1D, E, and F, the number of white blood cells (monocytes, lymphocytes, and granulocytes) present in PRP samples was significantly reduced after the 1st and 2nd centrifugation compared to the whole blood fraction. As expected, platelets gradually increased at each centrifugation step, being the final solution significantly filled with high levels of platelets, with the absence of red blood cells, and lower levels of white blood cells. Particularly, despite not detectable values for monocytes and lymphocytes, a residual number of granulocytes were seen in the sample collected from donor 3, after the 2nd step of centrifugation (Supplementary Fig. 1F). Therefore, the correct designation for the final enriched plasma solution obtained was Leukocyte-poor platelet-rich plasma (LP-PRP), as a significant reduction in Leucocytes (more than 2.5 × related to whole blood baseline) was observed in our PRP samples.

The pool of LP-PRP samples generated presented significantly higher levels of platelets (1429 ± 364 platelets/mm^3) in comparison with PPP control (38.55 ± 7.27 platelets/mm^3) (Supplementary Fig. 1B). This range in platelets/

mm^3 values, both for PPP and LP-PRP pools, was similar in the other pools that were obtained from the other blood donors (data not shown).

Activated Platelets Release BDNF

The stimulation with calcium chloride led to platelet degranulation, clearly evidenced by the formation of fibrin nets between platelets in LP-PRP samples activated (Fig. 1A). In these samples, the amount of BDNF released was almost twice as seen for activated PPP (LP-PRP: 65.07 ± 11.83 pg/mL; PPP: 36.96 ± 2.98 pg/mL). Furthermore, the amount of BDNF released by activated LP-PRP was at least 8 times higher in comparison with non-activated controls (LP-PRP: 7.52 ± 1.44 pg/mL; PPP: 7.78 ± 0.88 pg/mL; Fig. 1B).

The Supernatant Harvested from Activated LP-PRP Decreases M1 Polarization Via the TrkB Receptor

BMDM cells stimulated with LPS/IFN-γ exhibited robust M1 phenotype, confirmed by significant mRNA *Nos-2* expression related to control (Fig. 2A). This M1 phenotype was significantly decreased when the SLPPRP was applied in the culture medium, downregulating *Nos-2* mRNA levels, being equivalent to non-stimulated cells (Fig. 2A). Interestingly, it was observed that the pre-treatment with ANA-12, a TrkB antagonist, blocked the effect of SLPPRP on *Nos-2* mRNA expression (Fig. 2A). This suggests that the TrkB receptor can be involved in this suppression of M1 polarization induced by SLPPRP. However, although *Nos-2* was effectively modulated by SLPPRP, the levels of *Arg-1* mRNA expression remained unaltered (Fig. 2C). Likewise, the mRNA levels related to M1 and M2 phenotypes in the complementary controls adopted in this assay were similar to non-stimulated cells (Fig. 2B and D; ANA-12 and Vehicle groups).

TrkB Receptor Mediates the Effects of LP-PRP on the Joint Injury Induced in the MIA Model

Typical OA-like injuries were detected in knee joints of rats previously injected with MIA. In these animals, along with cartilage breakdown, the subchondral bone was exposed in focal areas (Fig. 3B, red arrows; and 3B-II for high magnification) followed by focal reactive bone-marrow lesions (BMLs) (Fig. 3B, asterisk symbol). All these findings were absent in the saline group that presented healthy and intact morphology of the joint (Fig. 3A, and A-I for high magnification). The injection of LP-PRP could mitigate the OA-like features induced by MIA (Fig. 3C, and C-III for high magnification). The animals that were submitted to the LP-PRP therapeutic protocol showed an intact articular cartilage with the absence of fissures. Some fibrillogenesis (Fig. 3C-black arrows) and focal BMLs were detected (Fig. 3C-asterisk) in animals of this group. However, these features were less extent in comparison with MIA group. The debilitated state observed for MIA group was similarly replicated on animals that received the TrkB antagonist followed by LP-PRP injection (Fig. 3D, and D-IV for high magnification). This indicates that the TrkB receptor could be mediating the LP-PRP effects in mitigate joint injury promoted in MIA model. The histopathological features seen in animals of ANA-12 or ANA-12 Vehicle groups were similar to those presented in MIA group (Fig. 3E, F; V and VI for high magnification). Lastly, the OARSI score analysis highlighted the qualitative data presented by all groups (Fig. 3G). The LP-PRP treatment could lower the histopathological score induced by MIA, where the ANA-12 + LP-PRP, ANA-12, and ANA-12

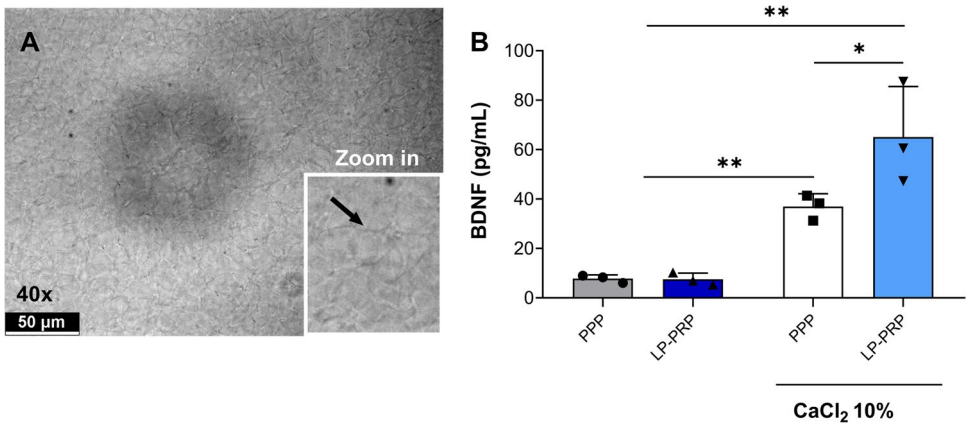

Fig. 1 Activated platelets release BDNF. Platelets from LP-PRP samples form fibrin nets after being exposed to 10% $CaCl_2$, indicating an activated state (**A**). BDNF amounts in the supernatant collected from activated LP-PRP samples were significantly higher in comparison to activated PPP and non-activated controls (**B**). Results are shown as Mean ± Standard Deviation. Symbols * and ** indicate respectively, $P < 0.05$ and $P < 0.01$, for comparison between highlighted groups. One-way ANOVA, Tukey post-hoc test.

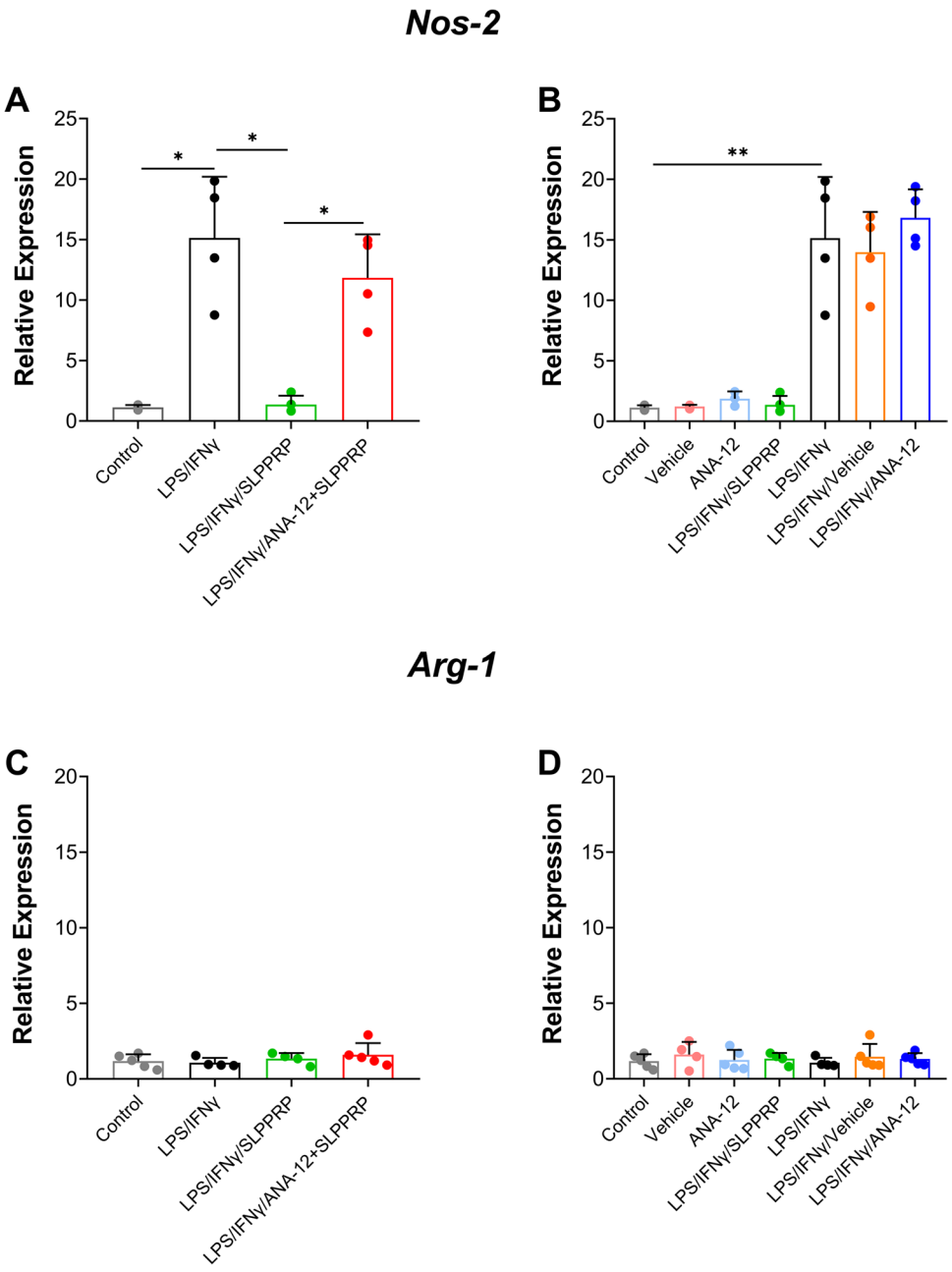

Fig. 2 LP-PRP effects on M1-like phenotype induced by LPS/IFN-γ are mediated by the TrkB receptor. BMDM cells stimulated with LPS/IFN-γ exhibited marked *Nos-2* mRNA expression in comparison with non-stimulated cells (**A**; control group). This marked *Nos-2* expression is significantly reduced in BMDM cells that were initially primed with LPS/IFN-γ 2 h in advance and then treated with SLPPRP (**A**; LPS/IFN-γ/SLPPRP vs LPS/IFN-γ group). The effects of SLPPRP at M1-like phenotype induced by LPS/IFN-γ are significantly reversed by TrkB receptor antagonist, ANA-12 (A, LPS/IFN-γ/ANA-12 + SLPPRP vs LPS/IFN-γ/SLPPRP group), suggesting TrkB dependent mechanism for LP-PRP suppression of M1-phenotype driven by LPS/IFN-γ stimulation. Although effective modulation was seen for *Nos*-2 with SLPPRP treatment, the levels of Arg-1 mRNA expression remained unaltered (**C**). The mRNA levels related to M1 and M2 phenotypes in the complementary controls adopted were like non-stimulated cells (**B** and **D**; ANA-12 and Vehicle groups). Results are shown as Mean ± Standard Deviation. Symbols * and ** indicate respectively, $P < 0.05$ and $P < 0.01$ for comparison between highlighted groups. One-way ANOVA, Tukey post-hoc test.

vehicle groups were not statistically different from animals that were only injected with MIA.

OA-Like Injuries in MIA-Injected Joints are Followed by Neuronal Injury in DRGs and Mitigated by LP-PRP

The OA-like injuries in knee joints of rats previously injected with MIA were followed by a substantial increase in ATF-3 staining in DRG neurons (Fig. 4A, B, and G). The LP-PRP therapeutic protocol was able to counteract this neuronal injury promoted by MIA, while the TrkB antagonism paired with LP-PRP injection led to a similar outcome as observed in DRGs from MIA animals (Fig. 4B, C, D, and G). No statistical difference was observed in the percentage of ATF-3-labeled neurons in animals previously injected with MIA and treated with ANA-12 or its vehicle alone in comparison with MIA control, indicating similar patterns of neuronal injury between these groups (Fig. 4B, E, F, and G).

Taken together, the data provided in this subset of results complement the joint-histopathology findings and show an interplay between degenerative events occurring at the articular space and the predicted sensorial damage at the DRG, where therapies such as PRP that modulate these

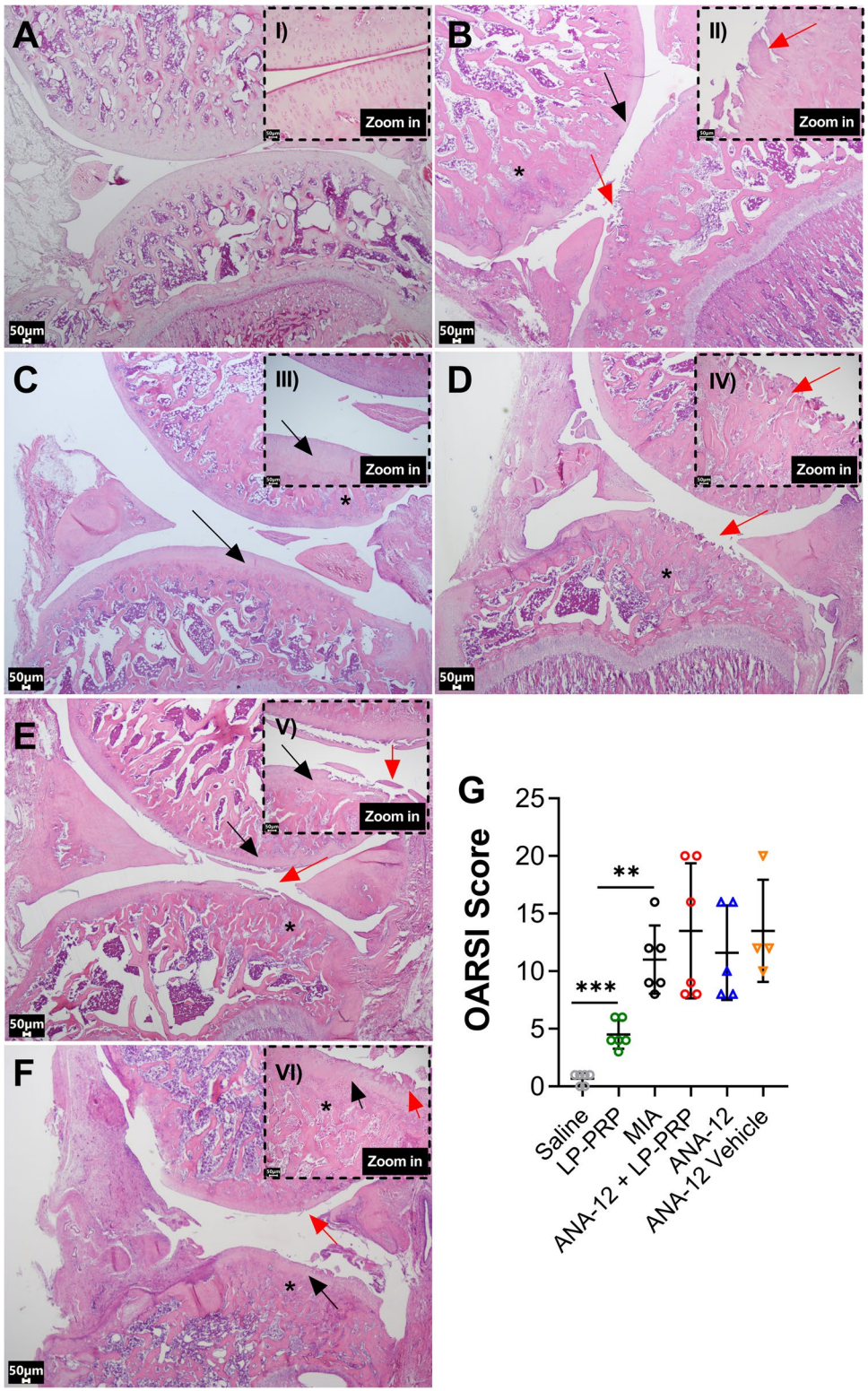

Fig. 3 TrkB receptor mediates the effects of LP-PRP on the joint injury induced in the MIA model. Typical OA-like injuries were detected in knee joints of rats previously injected with MIA in comparison with control (**A**, **B**). The injection of LP-PRP mitigates the OA-like features induced by MIA (**C**), where the debilitated state observed in MIA-injected joints was similarly replicated on animals that received TrkB antagonist followed by LP-PRP injection (**D**). The histopathological features seen in animals that were previously injected with MIA and treated with ANA-12 alone or its vehicle were like those presented by the MIA group as well (**E**, **F**). The OARSI score analysis (**G**) shows quantitative data from all groups, highlighting the decreased histopathological score presented by the LP-PRP group, and as in the MIA group, similar values were observed for ANA-12 + LP-PRP, ANA-12, and ANA-12 vehicle groups. Results are shown as Mean ± Standard Deviation. Symbols ** and *** indicate respectively, $P < 0.01$ and $P < 0.001$ for comparison between highlighted groups. One-way ANOVA, Tukey post-hoc test. Images at 2× magnification (**A**–**F**). Images at 20× magnification (I and II). Images at 10× magnification (III-VI). Red arrows—Cartilage breakdown or subchondral bone exposure; Black arrows – Fibrillogenesis; Asterisk – Focal bone marrow reactive lesions (BMLs).

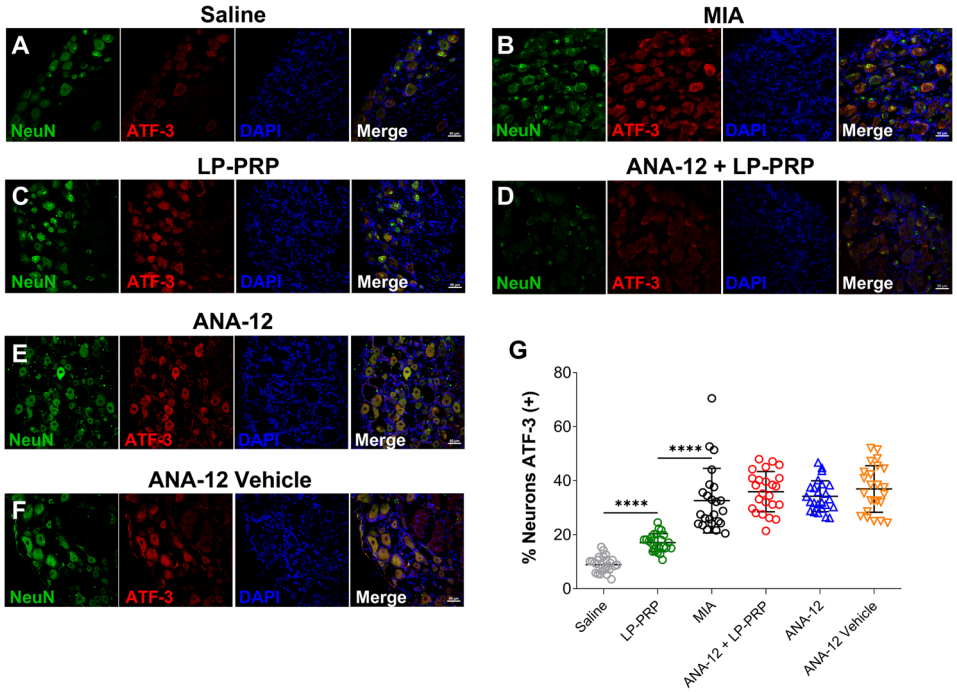

Fig. 4 MIA-induced neuronal injury is mitigated by LP-PRP with potential implications of the TrkB receptor. Rats' knee joints previously injected with MIA (2 mg; 25 µL; intra-articular) were followed by a substantial increase in ATF-3 staining in DRG neurons in comparison with saline controls (**A**, **B**, and **G**) at day 21. The LP-PRP therapeutic protocol decreased this neuronal injury promoted by MIA, while the TrkB antagonism (ANA-12; 100 µM; 25 µL; intra-articular) paired with LP-PRP injection led to a similar outcome as observed in DRGs from MIA animals (**B**, **C**, **D**, and **G**). No statistical difference is seen in the percentage of ATF-3-labeled neurons in animals previously injected with MIA and treated with ANA-12 (100 µM; 25 µL; intra-articular) or its vehicle alone 1% DMSO solution; 25 µl; intra-articular) in comparison with MIA control, showing similar patterns of neuronal injury between these groups (**B**, **E**, **F**, and **G**). Results are shown as Mean ± Standard Deviation. Results are shown as Mean ± Standard Deviation. Symbol **** indicates $p < 0.0001$ for comparison between highlighted groups. Symbol NS indicates a non-significant comparison between the groups highlighted. One-way ANOVA, Tukey post-test. Images at 20× magnification and scale bar at 50 µm.

tissue-damage events will eventually interfere with the sensory outcome as well, especially neuronal injury.

Mitigation Promoted by LP-PRP on TNF-α Concentration in MIA-OA Joints Involves the Participation of the TrkB receptor

Blocking the TrkB receptor led to an increase of TNF-α release in joint homogenate from OA animals, as seen in ANA-12 + LP-PRP and in ANA-12 groups (Fig. 5A). The LP-PRP protocol reduces TNF-α (Fig. 5B), and a slight reduction was noticed for IL-1β titers, although non-significant when compared to the ANA-12 and ANA-12 + LP-PRP groups (Fig. 5C and D). This result suggests an endogenous role of the TrkB receptor by modulating TNF-α concentrations in MIA-induced osteoarthritic joints. Once this same event was replicated in the presence of LP-PRP, it is reasonable to consider that one of the mechanisms by which LP-PRP promotes TNF-α decrease on MIA-OA joints involves the participation of the TrkB receptor.

The Effects of LP-PRP on Joint Hyperalgesia Induced by MIA Require TrkB Receptor Participation

MIA injection into knee joints of rats promoted long-lasting joint mechanical hyperalgesia, as seen by the decrease of joint flexion mechanical thresholds starting at day 3 and persisting until day 21 post-MIA injection (Fig. 6A). The LP-PRP treatment could significantly reduce the MIA-joint hyperalgesia at days 7 and 14 after MIA injection (Fig. 6A). The analyzed area under the curve (AUC) of the LP-PRP group showed a significant increase in comparison with the MIA group. This suggests differences in time-displacement recovery regarding mechanical thresholds between these two groups (Fig. 6B), implying a gain in recovery from

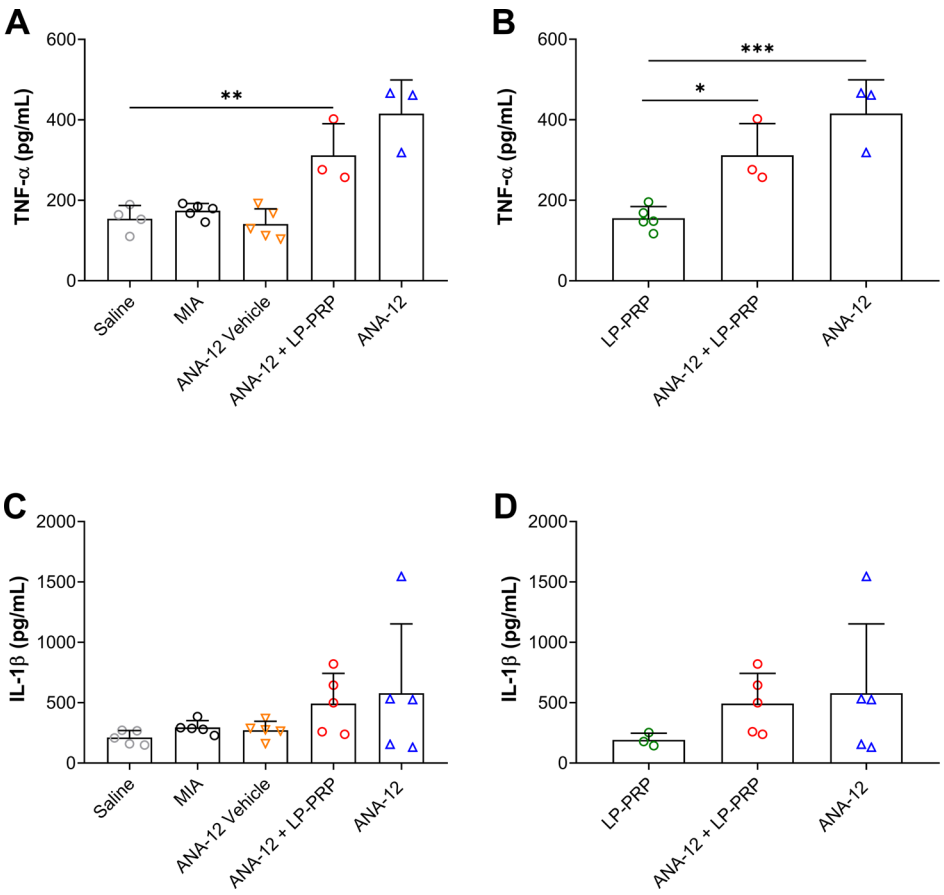

Fig. 5 LP-PRP decreases in the TNF-α concentrations in MIA-OA joints require the participation of the TrkB receptor. **A** and **B** The blockade of the TrkB receptor led to an increase in TNF-α concentrations in the joint homogenate from animals previously injected with MIA (2 mg; 25 µL; intra-articular). The amount of TNF-α cytokine in ANA-12 and ANA-12 + LP-PRP groups was significantly different from the other groups analyzed, especially MIA and LP-PRP. **C** and **D** No statistical difference was observed between groups regarding IL-1β concentrations in the samples analyzed. Results are shown as Mean ± Standard Deviation. Symbols *, **, and *** indicate respectively, $P < 0.05$, $P < 0.01$, and $P < 0.001$ for comparison between highlighted groups. One-way ANOVA; Tukey post-hoc test.

joint-flexion mechanical thresholds produced by LP-PRP injection.

The effects of LP-PRP treatment at the hyperalgesic joints were reversed in animals where TrkB receptor was blocked, such as seen in ANA-12 + LP-PRP group (Fig. 6C). This result suggests that the TrkB receptor is involved in the functional outcome promoted by LP-PRP in MIA-OA joints, especially for the joint flexion mechanical threshold recovery (Fig. 6C and D). In addition, the TrkB antagonism in animals previously injected with MIA, to investigate an endogenous TrkB role in joint pain triggered by MIA, did not show differences in joint flexion mechanical thresholds comparing with OA controls just injected with MIA. However, as observed in (Fig. 6C and D) the ANA-12 group displayed significant different joint flexion thresholds in comparison with LP-PRP treated animals.

The Improvement on Gait Dysfunction Induced by LP-PRP on MIA-OA Model Requires TrkB Receptor Participation

The injection of MIA into the knee joints led to a prominent debilitation state reflected by a significant gait dysfunction three days after the insult and lasting at least until day 21 post-MIA injection (Figures A, E, and I). The LP-PRP treatment could mitigate significantly the alterations triggered by MIA in the spatiotemporal parameters *Max contact area* (Fig. 7A), *Print area* (Fig. 7E), and *Print width* (Fig. 7I). Additionally, compared to the MIA group in all these previously mentioned parameters, the LP-PRP displayed a significantly differences in AUC analysis (respectively in Fig. 7C, G, and K). Notably, these same gait improvements (Figures B, F, and J) and AUC (Fig. 7D, H, and L) were also observed in the LP-PRP group in comparison to the ANA vehicle, ANA-12, and ANA + LP-PRP group.

These results suggest a role of the TrkB receptor in biological activities exerted by LP-PRP in the joint compartment implied in gait performance, as changes in gait, especially related to spatiotemporal parameters, were followed by changes in AUC which infers differences in temporal pattern from time curves [46, 47]. In this sense, the results suggest that these changes in gait parameters might reflect time-dependent gain in joint function triggered by LP-PRP injection.

No significant changes in gait parameters were observed in animals injected with MIA and post-treated with ANA-12 or its vehicle in comparison with the MIA-OA control group (injected only with MIA; MIA group), or with ANA-12 + LP-PRP group (Fig. 7B–D; F–H; J–L).

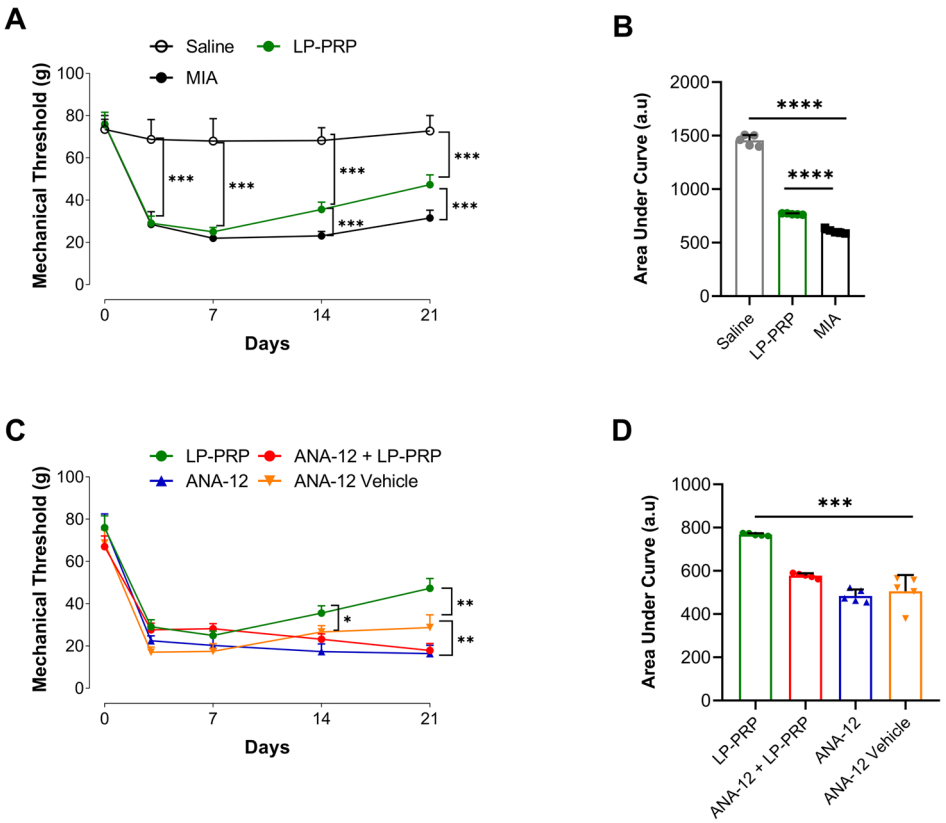

Fig. 6 The effects of LP-PRP on joint hyperalgesia induced by MIA require TrkB receptor participation. **A** The injection of MIA into rats' joints led to a long-lasting joint mechanical hyperalgesia evident throughout the significant decrease in the mechanical joint flexion thresholds 3 days after MIA intra-articular delivery (2 mg; 25 µL, at day 0). The LP-PRP protocol (25 µL; intra-articular) significantly mitigated the MIA-joint hyperalgesia at days 7 and 14 after MIA injection. **B** The analyzed area under the curve (AUC) between MIA and LP-PRP shows significant differences, suggesting a time-displacement recovery difference regarding mechanical thresholds between these two groups. **C** In animals where the TrkB receptor blockade was paired with LP-PRP protocol (ANA-12; 100 µM; 25 µL; days 7 and 14 after MIA; ANA-12 + LP-PRP group), the effects of LP-PRP at the hyperalgesic joints were reversed and animals presented a slight significant decrease in the mechanical thresholds in comparison with the vehicle controls. These events seen for the TrkB blockade on the LP-PRP protocol were replicated when we performed TrkB antagonism in animals previously injected with MIA. **D** The AUC analysis showed that the TrkB receptor blockade reversed the gain in time-displacement recovery induced by the LP-PRP protocol, as the AUC presented by the ANA-12 + LP-PRP group was significantly lower in comparison with the LP-PRP group. Results are shown as Mean ± Standard Deviation. Symbols *, **, *** and **** indicate respectively, $P < 0.05$, $P < 0.01$, $P < 0.001$ and $P < 0.0001$ for comparison between highlighted groups. **A** and **C** Two-way ANOVA; **B** and **D** One-way ANOVA; Tukey post-hoc test.

Discussion

This is the first work that aimed to analyze the implications of the BDNF and the Tropomyosin Kinease B (TrkB) receptor in the effects of PRP therapy in OA animals. Previous works showing the presence of BDNF in other sites rather than neuronal tissue and implicated in functional activities of platelets have been reported by Chacón-Fernández et al. [11], Fujimura et al. [48], and Le Blanc et al. [49].

Evolutionarily, the platelet system was conceived in mammals to control hemostasis, ensure the mitigation of vascular damage, and avoid bleeding and tissue injury [50]. In such reparative and physiological role, products such as ATP and calcium ions act as main agonists in platelet degranulation [28, 51]. We observed that the use of 10% $CaCl_2$ could stimulate platelet degranulation and BDNF release. Similar results were obtained by Le Blanc et al. [49], that suggest a plasmatic predominance in BDNF concentrations coming from activated platelets through a series of agonists such as ADP, collagen, calcium, and arachidonic acid.

Previous findings suggest that BDNF is stored in cytosol and at α-granules in platelets [11, 49]. These α-granules are structures that are present platelets plasmatic membrane and oscillations in intracellular calcium stores stimulate their exocytosis and content release [28]. As previously mentioned, different sets of molecules implicated in tissue injury signaling can trigger BDNF release in platelets [48, 49]. In this sense, studies regarding mechanisms involved on the docking and release of this neurotrophin in platelets will be of quite interest to elucidate if classical exocytosis

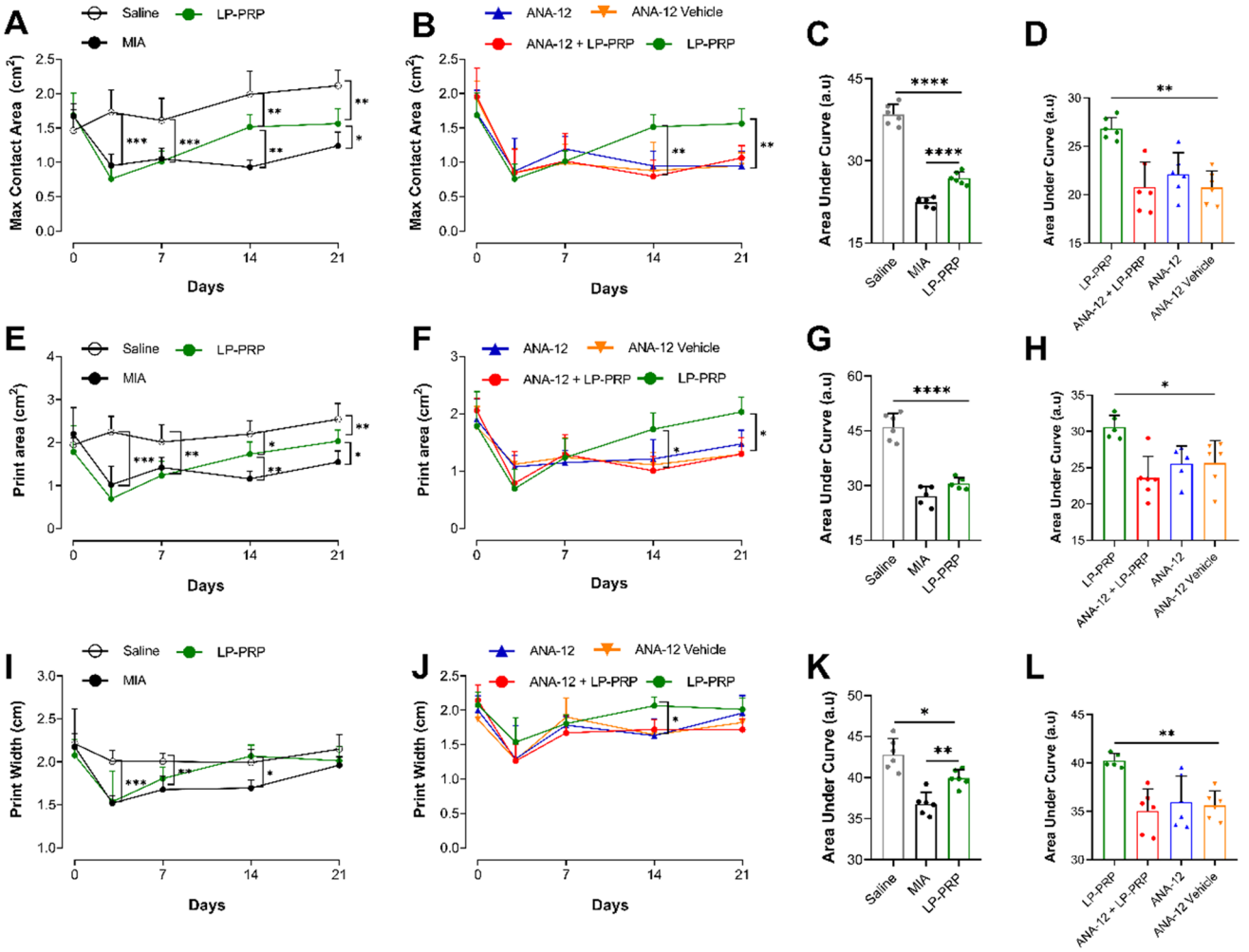

Fig. 7 The effects of LP-PRP on gait dysfunction induced by MIA require TrkB receptor participation. **A**, **E** and **I** MIA delivery (2 mg, 25 µL) on the knee joints from naive rats led to a prominent debilitation state reflecting significant gait dysfunction three days after the insult and lasting at least until day 21 after MIA intra-articular injection. The LP-PRP protocol (25 µL; intra-articular; days 7 and 14) could significantly mitigate the alterations led by MIA in the spatiotemporal parameters Max contact area, Print area, and Print width. **C** This gait improvement was also followed by a time-displacement recovery as shown by the significant differences between AUC present by LP-PRP in comparison with the MIA group. **D**, **H** and **L** The paired intra-articular delivery from the TrkB antagonist (ANA-12; 100 µM; 25 µL; days 7 and 14) with the LP-PRP protocol promoted a significant reversal both at gait and AUC altered by LP-PRP. No significant changes in gait parameters were observed in animals injected with MIA and post-treated intra-articularly with ANA-12 (ANA-12; 100 µM; 25 µL; days 7 and 14) or its vehicle (1%DMSO; 25 µL; days 7 and 14) in comparison with the OA control group (MIA group), or with ANA-12 + LP-PRP group. Results are shown as Mean ± Standard Deviation. Symbols *, **, *** and **** indicate respectively, $P < 0.05$, $P < 0.01$, $P < 0.001$ and $P < 0.0001$ for comparison between highlighted groups. **A** and **C** Two-way ANOVA; **B** and **D** One-way ANOVA; Tukey post-hoc test.

protein complexes that led to granule release in platelets, such as VAMP-8 and SNARE proteins, are also involved in BDNF release from platelet granules [28, 52].

Perhaps one of the most important interactions for tissue repair is the crosstalk between platelets and macrophages [53, 54]. Macrophages have an essential role in maintaining joint homeostasis and present a dynamic plasticity that can be modulated by platelets [7, 54, 55]. In this regard, platelets can release inflammatory cytokines such as IL-1β and TNF-α that trigger M1-phenotype in macrophages, typically known as inflammatory [56–58]. On the other hand, platelets also release Tumor growth factor beta (TGF-β) and Fibrinogen, that are known to trigger an M2-phenotype in macrophages, reported as anti-inflammatory [56–58].

Although macrophage polarization has been extensively mentioned as one of the primary mechanisms by which PRP improves tissue repair [7, 53], little is known about the role of BDNF in such therapeutic activity induced by PRP.

In our hands, BMDM cells that were polarized for a M1-like phenotype by LPS/IFN-γ had this event mitigated

by SLPPRP. Additionally, the effects of SLPPRP were reversed in the presence of TrkB receptor antagonist, suggesting a role of BDNF in the suppression of M1-phenotype induced by SLPPRP. Although the results suggest a preventive effect of SLPPRP, given the short time window between the stimulus and treatment, a study showed that in 1 h after the LPS insult, there is a substantial increase in iNOS expression, a M1-phenotype marker [59]. In this study the protein and mRNA levels of iNOS in macrophage cells persisted significantly altered for at least 24 h after stimulus [59]. Thus, our results suggest that SLPPRP would be acting in these M1-like cells to reprogram or counteract an inflammatory state, which TrkB receptor seems to be involved.

Despite significant modulation was seen by SLPPRP in M1-phenotype, no changes in *Arg-1* expression were detected, suggesting that no M2-like phenotype could be triggered by SLPPRP treatment. Indeed, the *in-vitro* time-course for M2-phenotype triggered by *Arg-1* modulation induced by PRP and its therapeutic derivatives such as LP-PRP and PRGF seems to occur in a timely manner, with significant levels of *Arg-1* mRNA being seen between 6 and 24 h after incubation [60–62]. Another possibility is that the anti-inflammatory cytokines and peptides present in non-activated plasma, that boosts PRP activity after injection, would not influence SLPPRP activity and thus limit our observations. In conclusion, the failure of SLPPRP in induce an M2-like phenotype in our experiments could be attributed to the earlier cells harvesting performed at the third hour after stimulus or due to an intrinsic activity of SLPPRP. At both cases, detectable changes in *Arg-1* message would require more time to be achieved.

The interaction between BDNF and TrkB receptor in neurons led to the activation of signaling cascades ruled by Phosphoinositide-3-Kinase (PI3K), Mitogen-Activated Protein Kinase (MAPK), Phospholipase C Gamma (PLCγ), and Guanosin Triphosphate Hydrolases (GTPases) enzymes that ultimately lead to cell growth, dendrite branching, cell survival and synaptic plasticity [63]. BDNF signaling through PI3K leads to further phosphorylation of AKT kinase inhibiting the intrinsic and extrinsic pathways and further neuronal apoptosis [63]. In macrophages, it is known that AKT isoforms 1 and 2 (AKT_1 and AKT_2, respectively) directly regulate macrophage polarization by modulating iNOS and Arg-1 expression [64]. The absence of AKT_1 in macrophages promotes hyperresponsiveness to LPS and increased iNOS gene expression, exacerbating M1 inflammatory response and further increase in IL-1β, TNF-α, and IL-6 cytokines. The opposite is observed in the absence of AKT_2, that leads to an exacerbation of anti-inflammatory response by upregulating Arg-1 [64]. Thus, it is possible that BDNF via TrkB receptor could regulate macrophage polarization through AKT signaling. However, more studies are required to confirm this hypothesis.

After sets of *in-vitro* experiments, we investigated the implications of the TrkB receptor in the repair activities induced by LP-PRP in OA animals.

The TrkB receptor is expressed in many cells of the joint compartment, such as synoviocytes, chondrocytes, osteoclasts, and osteoblasts [19, 65–68]. Although not directly linked with OA pathogenesis, BDNF via TrkB receptor have potential therapeutic activities through its anti-inflammatory [15], anti-apoptotic [63], antioxidant and modulation of autophagy [69] actions that could induce healing cascades in OA affected joints.

In our studies, an interesting decrease in knee joint injury followed by functional recovery of both joint-flexion mechanical thresholds and gait was observed after LP-PRP treatment. These mitigation on OA-like injuries are dependent on TrkB receptor, since the effects of LP-PRP, both at behavioral and tissue repair outcomes (joint and nerve injury) were significantly reversed in the presence of the selective TrkB antagonist, ANA-12.

As in humans, the OA model triggered by MIA in murine animals display similar pathological changes resulting from oxidative stress in joint cells, which leads to ongoing tissue catabolism, inflammation, cartilage breakdown, nerve injury, and chronic pain [70, 71]. These OA-like alterations are divided into an acute and late phase [71–73].

During the acute phase of MIA model, typically reported as inflammatory, an increase in cytokines such as IL-1β, TNF-α, IL-6, IL-8, and chemokines, such as CCL-2 are observed [70, 72–77]. In parallel, an enhancement on cell recruitment occurs in the knee joint, resulting on an increasing number of inflammatory cells such as macrophages, dendritic cells, neutrophils, and mast cells [77–79]. Particularly, a shifting to M1 profile is noticed in macrophages, driven by the massive released of tissue degradation products and cytokines that ultimately contribute to boost the late phase of MIA-OA model, looping the pro-inflammatory context and stablishing an ongoing tissue injury that sets a degenerative process [70, 75, 77, 80].

Following the acute phase, in the late stage of MIA model, known as chronic and degenerative, a decrease in the expression of enzymes linked with cell survival against oxidative damage, such as SOD-2 and Catalase, and increased expression of matrix metalloproteinases (MMP), such as MMP3 and 9, are observed [70, 74, 81, 82]. As this catabolic state goes by, the cell-death tied to a hyperactivity of MMPs led to cartilage breakdown and further sensitization of sensory fibers due to nerve injury of primary afferent terminals in subchondral bone. The sensitization of joint nociceptors is also driven by inflammatory products that could be present on synovial fluid such as IL-1β, TNF-α, IL-6 and NGF [70, 77, 83].

Given that joint histological changes triggered by MIA are dictated by a series of pathological mechanisms, our

results suggest that LP-PRP would be acting in the inflammation and degeneration cascades induced by MIA to antagonize tissue injury and improve repair at the affected joints, thus, resulting in substantial changes on joint morphology with the therapeutic protocol. In this regard, studies have shown interesting mechanisms by which PRP could promote joint repair in OA and impact histological changes.

Previous works reported that PRP in-vitro promotes i) cellular differentiation of chondrocytes via regulation of cyclins B1, D1, and E2, ii) decrease apoptotic signaling induced by caspase-3 and p53, and iii) alleviates ROS-induced oxidative damage triggered by IL-1β [22, 84, 85]. Importantly, chondrocyte differentiation is a key activity to boost tissue matrix peptides synthesis and further mitigate joint catabolism triggered in OA [86]. Interestingly, PI3K and AKT signaling that are activated by BDNF-TrkB interaction have a role in chondrocyte terminal differentiation in murine embryos [87].

Aside from in-vitro activities, some studies also have shown that PRP treatment mitigates OA joint injuries by decreasing the expression of MMPs 1, 3, and 13 [22, 84, 85]. In interfering with the activity of these metalloproteinases, PRP alleviated tissue degeneration and the ongoing joint damage that leads to chronic inflammation in OA. Interestingly, an interaction of BDNF and Runx-2, a transcriptional factor known to regulate chondrogenesis and mitigate OA cartilage injury by downregulating MMP-13 and other matrix metalloproteinases as Adamts-5, is described in a non-OA animal model [88].

It has been widely reported that therapeutic approaches capable of interfering with oxidative damage and modulate autophagy mechanisms in chondrocytes can improve tissue healing in OA joints [89–91]. Considering the BDNF-TrkB interaction, activities such as decrease in ROS tissue damage towards modulation of the SOD-2 enzyme [65, 92, 93] and $FOXO_3$ protein signaling [94] had been previously reported. The FOXO proteins complex is involved in cell defense against oxidative stress and modulation of autophagy genes such as *Sesn3* and *Bnip3* that prevent chondrocyte apoptosis and cartilage aging [91].

In summary, is reasonable to suggest that the interaction between BDNF-TrkB arising after LP-PRP injection and further platelet degranulation has as one of main therapeutic axis the attenuation of oxidative stress triggered in MIA-OA model [70, 81, 82]. Complementary, the shared anti-inflammatory profile induced by PRP and BDNF, such as a decrease in inflammatory IL-1β/TNF-α and enhancement of the anti-inflammatory IL-10/IL-4 cytokine axis [15, 95] could be contributing to a suppression on macrophage-M1 profile, and thus, a decrease in further ongoing-tissue injury, given the initiation of therapeutic protocol with LP-PRP at day 7 after MIA insult, which comprehends the transitioning period between the acute phase and chronic phase of MIA-OA model [70, 75].

In this sense, this downward on tissue inflammatory and catabolic state clearly provided by LP-PRP and BDNF-TrkB interaction reflects the findings in our tissue pathology assays (joint and DRG) and corroborates with our behavior results: OA-like injuries are attenuated in the presence of LP-PRP, where its therapeutic activities are reversed in the presence of TrkB antagonist. The importance of these BDNF-TrkB biological activities for joint repair are highlighted at the functional (gait and pain behavior) outcomes obtained in presence and absence of the TrkB antagonist.

Joint nociceptive neurons typically evoke action potentials in response to stimuli that breakthrough the tissue's physiological working range [96–99]. Thus, when a static or dynamic pressure stimulus, such as intense pressure, sharp rotation, or twisting, exceeds the joint baseline resistance, the result is an avoidance of harmful motion, withdrawal of, and preservation of the affected limb [96, 97, 99].

Although some murine models shown an overlap between antalgic gait and pain behavior such as seen in diabetic neuropathy [100], a study have shown no reversal of antalgic gait parameters in presence of analgesics, especially in CFA and spared nerve injury pain models [101]. Particularly for MIA-OA models, there is still no concise data, where some studies report none to mild changes in gait after MIA [102] and some seen markable joint dysfunction regarding spatiotemporal parameters at the acute and late phase of the model [73, 103–105]. In these studies, it is a common understanding that joint dysfunction triggered by MIA is followed by changes in print-area, print length and print width parameters [73, 103–105].

In our experiments, the LP-PRP therapeutic protocol was able to increase the max contact area as well as print-length, and print-width gait parameters at day 14 and 21st after MIA injection. These improvements in gait were also followed in joint mechanical thresholds and reversed in the presence of TrkB antagonist, ANA-12. Interestingly, the animals in the ANA-12 and ANA-12 + LP-PRP groups displayed significantly decreased joint-flexion mechanical thresholds in comparison with both OA controls treated with antagonist vehicle (ANA-12 vehicle group). However, despite this worsening in joint-flexion mechanical thresholds, this event was not replicated in the gait parameters analyzed.

It is important to note that although there is some significant interdependence between antalgic gait and mechanical thresholds linked with joint injury (such as joint flexion thresholds or secondary allodynia), these parameters might not strictly follow covariance over time [73, 73, 102, 104].

In this sense, joint nociceptive afferents have prominent response to noxious flexion or twisting stimuli [96–99]. Although it seems plausible that the nerve injury tied to the persistent inflammatory phenotype driven by increased

TNF-α in ANA-12 and ANA-12 + LP-PRP groups would imply an increase in gait behavior related to joint noxious dysfunction, the animal's ability to adapt joint motion to preserve normal gait would bias our conclusions in showing no changes related to spatiotemporal parameters, at least at the endpoint measurements. Another possibility is that the antalgic gait seen in the MIA-OA model could be related to a significant impairment in joint mechanobiology properties that limit joint movement and further proper animal ambulation. Thus, this impairment would be more significant in the model's early phase due to an inflammatory input linked with swelling and joint sensitization. The gait alterations would be resolved as the inflammatory event decreases and acquires a latent characteristic, and the pain phenotype is mainly related to the ectopic activity of primary afferent neurons. In such ectopic activity, the nociceptive background would rely on nerve injury triggered in the model, where nociception and pain behavior would be achieved primarily through induction of joint flexion [99, 106]. In addition, the nerve injury seen mechanistically by increasing on ATF-3 expression in dorsal root ganglia neurons and implicated in joint nociceptive response can be associated with a persistent plasticity of these cells triggered by massive release of inflammatory peptides in the early phase of MIA or due to a mechanical injury of peripheral terminals present at joint capsule and subchondral bone [107, 108]. Of note, chemical (inflammatory cytokines and peptides) or mechanical (chronic constriction, axotomy) injury are primarily mechanisms involved in ATF-3 increase on the DRG [109–111].

Lastly, the improvements in joint performance by LP-PRP could be attributed to a shift in inflammation profile driven by this therapeutic after injection. This alternate in inflammatory and degenerative profile would be likely associated with a downregulation activity in macrophage M1-profile, mitigation in tissue catabolism and preservation in joint integrity that ultimately led to a decrease in inflammation and nerve injury of nociceptive afferents. These biological activities seem to involve an interaction between BDNF and TrkB receptors with implications in functional aspects as well, once both changes in histopathological, molecular, and pain phenotype evoked by LP-PRP were reversed in presence of TrkB antagonist [7, 11–13, 15, 19, 22, 28, 48–62, 64–85, 87, 88, 91–104, 106–126].

Conclusions and Study Limitations

Although the search for an effective drug in OA remission and chronic pain remains a challenge, our results support the use of PRP as a therapy for pain control and joint repair. Through behavioral and molecular experiments, the data presented in this work clarifies the discussion about the role of growth factors, particularly BDNF, in joint homeostasis.

The clinical relevance of neurotrophins in non-neuronal tissues, particularly for joint homeostasis, come with data from pre-clinical studies that had shown expression of TrkA (NGF) and TrkB (BDNF) receptors in synovium, bone, and cartilage tissue [65, 66, 127]. Notably, genomic alterations that lead to a dysfunction in these receptors have as an outcome dwarfism, insensitivity to pain and arthritic phenotype [66, 128, 129]. These disease conditions are commonly attributed to the anabolism and sensory perception properties, particularly from BDNF and NGF, that maintain bone and joint development as well as regulate joint proprioception and pain signaling [128, 130].

There is an increase interest in pharmacological approaches capable of regulating neurotrophins activity in osteoarthritic joints, particularly, NGF [130, 131]. However, although anti-NGF therapies appear to be effective in mitigate joint pain in OA models, no improvements in cartilage damage score were evidenced in a range of studies [131]. In this sense, our approach with LP-PRP gives some advantages once we notice mitigation of joint injury and pain behavior with the therapeutic protocol adopted in the study. The behavioral and tissue damage outcomes obtained with TrkB blockade paired or not with LP-PRP injections highlights the importance of BDNF-TrkB interaction to regulate inflammation and joint repair, where increase bioavailability can be achieve with LP-PRP therapy to provide better disease outcomes.

Despite platelets also stored in their granules Pro-BDNF protein, it is well understood that platelet activation by a series of agonists, such as ADP, collagen, calcium, and arachidonic acid, is followed only by the release of BDNF [49]. However, the residual amount of Pro-BDNF in plasma that does not originate from activated platelets can be one of the reasons why we detected limited improvements in tissue pathology and further joint function. Secondly, we acknowledge that some anesthetics, such as ketamine, decrease platelet membrane fluidity, interfering with their degranulate function [132, 133]. Once we used ketamine for terminal anesthesia and blood withdrawal for plasma retrieval, the PRP quality may have decreased, and such an event would have impacted our experimental findings. However, it is still unknown if anesthetics such as ketamine directly impact therapeutic outcomes induced by PRP.

The main goal of this study was to investigate the functional outcome of platelet BDNF in an osteoarthritis model, we directed our assays to analyze the contributions of this neurotrophin in biological activities of PRP in a pre-clinical OA murine model that mimics both inflammatory and degenerative state of the disease. We acknowledge that the study was conducted only in male animals and further investigation needs to be addressed to confirm if similar mechanisms regarding the role of BDNF-TrkB interaction in joint homeostasis can be replicated in females as well.

Lastly, we suggest a role of TrkB receptor in joint repair activities induced by PRP therapy and in the endogenous control of joint homeostasis given the results obtained in our endpoint measurements. However, more studies with longer follow-ups (more than 21 days), using other OA models, and with tissue-specific knockouts need to be addressed to unravel additional mechanisms regarding the role of BDNF in osteoarthritis [65, 66, 127–131, 131].

Supplementary Information The online version contains supplementary material available at https://doi.org/10.1007/s10753-024-02072-9.

Acknowledgements The authors gratefully acknowledge the Laboratories of Nerve Regeneration, of Histology at the Institute of Biology (IB; UNICAMP), the Laboratory for the Development of Biotechnological Processes at the School of Chemical Engineering (FEQ; UNCAMP), and the National Institute of Science and Technology on Photonics Applied to Cell Biology (INFABIC) for technical support.

Authors' Contributions KFM: conceptualization, methodology, validation, formal analysis, investigation, writing-original draft, writing—review & editing, visualization, and funding acquisition; DMS, CCF: writing-original draft, writing—review & editing; JBP, ALLO, MOP, NSC, CMN, CRRS: methodology; investigation; formal analysis; writing—review & editing; SRC, CRS, CHT: resources, writing—original draft, writing—review & editing; CAP: conceptualization, resources, writing—original draft, writing—review & editing manuscript, project administration, and funding acquisition.

Funding The present study was supported by grants awarded from the following Brazilian Research Institutes: Higher Education Personnel Improvement Coordination – (CAPES—Financing Code 001) and the Fundação de Amparo à Pesquisa do Estado de São Paulo (FAPESP—process 2018/10205-2) for scholarships and financial support essential to the development of the study.

Data Availability The datasets generated during the current study are available from the corresponding authors upon reasonable request.

Declarations

Ethics Approval and Consent to Participate The experiment was approved by the Ethics Committee on the Use of Animals (CEUA) for protocols 4706-1 and 4834-1A on November 9th, 2017. All experiments were conducted and performed according to the guidelines of the Brazilian National Council for Animal Experimentation Control (CONCEA).

Competing Interests The authors declare no competing interests.

References

1. Suri, Pradeep, David C. Morgenroth, and David J. Hunter. 2012. Epidemiology of osteoarthritis and associated comorbidities. *PM&R* 4: S10–S19. https://doi.org/10.1016/j.pmrj.2012.01.007. (Elsevier Inc.).
2. Wallace, Ian J., Steven Worthington, David T. Felson, Robert D. Jurmain, Kimberly T. Wren, Heli Maijanen, Robert J. Woods, and Daniel E. Lieberman. 2017. Knee osteoarthritis has doubled in prevalence since the mid-20th century. *Proceedings of the National Academy of Sciences* 114: 201703856. https://doi.org/10.1073/pnas.1703856114.
3. Hunter, David J., and Sita Bierma-Zeinstra. 2019. Osteoarthritis. *The Lancet* 393: 1745–1759. https://doi.org/10.1016/S0140-6736(19)30417-9.
4. Thakur, Matthew, Anthony H. Dickenson, and Ralf Baron. 2014. Osteoarthritis pain: Nociceptive or neuropathic? *Nature Reviews Rheumatology* 10: 374–380. Nature Publishing Group. https://doi.org/10.1038/nrrheum.2014.47.
5. Thakur, M., J. M. Dawes, and S. B. McMahon. 2013. Genomics of pain in osteoarthritis. *Osteoarthritis and Cartilage* 21: 1374–1382. Elsevier. https://doi.org/10.1016/j.joca.2013.06.010.
6. Martel-Pelletier, Johanne, Andrew J. Barr, Flavia M. Cicuttini, Philip G. Conaghan, Cyrus Cooper, Mary B. Goldring, Steven R. Goldring, Graeme Jones, Andrew J. Teichtahl, and Jean-Pierre. Pelletier. 2016. Osteoarthritis. *Nature Reviews Disease Primers* 2: 16072. https://doi.org/10.1038/nrdp.2016.72.
7. Andia, Isabel, and Nicola Maffulli. 2013. Platelet-rich plasma for managing pain and inflammation in osteoarthritis. *Nature Reviews Rheumatology* 9: 721–730. Nature Publishing Group. https://doi.org/10.1038/nrrheum.2013.141.
8. Andia, Isabel, and Nicola Maffulli. 2019. Blood-derived products for tissue repair/regeneration. *MDPI*. https://doi.org/10.3390/books978-3-03921-861-5.
9. Bansal, Himanshu, Jerry Leon, Jeremy L. Pont, David A. Wilson, Anupama Bansal, Diwaker Agarwal, and Iustin Preoteasa. 2021. Platelet-rich plasma (PRP) in osteoarthritis (OA) knee: Correct dose critical for long term clinical efficacy. *Scientific Reports* 11: 3971. https://doi.org/10.1038/s41598-021-83025-2.
10. Simental-Mendía, Mario, Daniela Ortega-Mata, and Carlos A. Acosta-Olivo. 2023. Platelet-rich plasma for knee osteoarthritis: What does the evidence say? *Drugs & Aging* 40: 585–603. https://doi.org/10.1007/s40266-023-01040-6.
11. Chacón-Fernández, Pedro, Katharina Säuberli, Maria Colzani, Thomas Moreau, Cedric Ghevaert, and Yves Alain Barde. 2016. Brain-derived neurotrophic factor in megakaryocytes. *Journal of Biological Chemistry* 291: 9872–9881. https://doi.org/10.1074/jbc.M116.720029.
12. Yamamoto, Hirotaka, and M.E. Gurney. 1990. Human platelets contain brain-derived neurotrophic factor. *The Journal of Neuroscience* 10: 3469–3478. https://doi.org/10.1523/JNEUROSCI.10-11-03469.1990.
13. Burnouf, Thierry, Ya.-Po. Kuo, David Blum, Sylvie Burnouf, and Su. Chen-Yao. 2012. Human platelet concentrates: A source of solvent/detergent-treated highly enriched brain-derived neurotrophic factor. *Transfusion* 52: 1721–1728. https://doi.org/10.1111/j.1537-2995.2011.03494.x.
14. Kilian, Olaf, Sonja Hartmann, Nicole Dongowski, Srikanth Karnati, Eveline Baumgart-Vogt, Frauke V. Härtel, Thomas Noll, Reinhard Schnettler, and Katrin Susanne Lips. 2014. BDNF and its TrkB receptor in human fracture healing. *Annals of Anatomy - Anatomischer Anzeiger* 196: 286–295. Elsevier GmbH. https://doi.org/10.1016/j.aanat.2014.06.001.
15. Calabrese, Francesca, Andrea C. Rossetti, Giorgio Racagni, Peter Gass, Marco A. Riva, and Raffaella Molteni. 2014. Brain-derived neurotrophic factor: A bridge between inflammation and neuroplasticity. *Frontiers in Cellular Neuroscience* 8: 1–7. https://doi.org/10.3389/fncel.2014.00430.
16. Sariola, H. 2001. The neurotrophic factors in non-neuronal tissues. *Cellular and Molecular Life Sciences* 58.
17. Hong, Jun Hee, Hyoung Min Park, Kyung Hee Byun, Bong Hee Lee, Woong Chol Kang, and Goo Bo Jeong. 2014. BDNF expression of macrophages and angiogenesis after myocardial infarction. *International Journal of Cardiology* 176: 1405–1408. Elsevier Ireland Ltd. https://doi.org/10.1016/j.ijcard.2014.08.019.

18. Simão, Adriano Prado, Vanessa Amaral Mendonça, Tássio Málber De Oliveira. Almeida, Sérgio Antunes. Santos, Wellington Fabiano Gomes, Candido Celso Coimbra, and Ana Cristina Rodrigues. Lacerda. 2014. Involvement of BDNF in knee osteoarthritis: The relationship with inflammation and clinical parameters. *Rheumatology International* 34: 1153–1157. https://doi.org/10.1007/s00296-013-2943-5.
19. Hutchison, Michele R. 2012. BDNF alters ERK/p38 MAPK activity ratios to promote differentiation in growth plate chondrocytes. *Molecular Endocrinology* 26: 1406–1416. https://doi.org/10.1210/me.2012-1063.
20. Papathanassoglou, Elizabeth D.E.., Panagiota Miltiadous, and Maria N. Karanikola. 2015. May BDNF Be implicated in the exercise-mediated regulation of inflammation? Critical review and synthesis of evidence. *Biological Research for Nursing* 17: 521–539. https://doi.org/10.1177/1099800414555411.
21. Zhu, Y., M. Yuan, H.Y. Meng, A.Y. Wang, Q.Y. Guo, Y. Wang, and J. Peng. 2013. Basic science and clinical application of platelet-rich plasma for cartilage defects and osteoarthritis: a review. *Osteoarthritis and Cartilage* 21: 1627–1637. Elsevier Ltd. https://doi.org/10.1016/j.joca.2013.07.017.
22. Chiou, Chi-Sheng, Chi-Ming Wu, Navneet Kumar Dubey, Wen-Cheng Lo, Feng-Chou Tsai, Tran Dang Xuan Tung, Wei-Ching Hung, Wei-Che Hsu, Wei-Hong Chen, and Win-Ping Deng. 2018. Mechanistic insight into hyaluronic acid and platelet-rich plasma-mediated anti-inflammatory and anti-apoptotic activities in osteoarthritic mice. *Aging* 10: 4152–4165. https://doi.org/10.18632/aging.101713.
23. Krajewska-Włodarczyk, Magdalena, Agnieszka Owczarczyk-Saczonek, Waldemar Placek, Adam Osowski, and Joanna Wojtkiewicz. 2018. Articular cartilage aging-potential regenerative capacities of cell manipulation and stem cell therapy. *International Journal of Molecular Sciences* 19: 623. https://doi.org/10.3390/ijms19020623.
24. Duan, Ran, Hui Xie, and Zheng-Zhao. Liu. 2020. The Role of Autophagy in Osteoarthritis. *Frontiers in Cell and Developmental Biology* 8: 1–9. https://doi.org/10.3389/fcell.2020.608388.
25. Armiento, Angela R., Mauro Alini, and Martin J. Stoddart. 2019. Articular fibrocartilage - Why does hyaline cartilage fail to repair? *Advanced Drug Delivery Reviews* 146: 289–305. The Authors. https://doi.org/10.1016/j.addr.2018.12.015.
26. Eming, Sabine A., Thomas A. Wynn, and Paul Martin. 2017. Inflammation and metabolism in tissue repair and regeneration. *Science* 356: 1026–1030. https://doi.org/10.1126/science.aam7928.
27. Andia, Isabel, Eva Rubio-Azpeitia, and Nicola Maffulli. 2015. Platelet-rich plasma modulates the secretion of inflammatory/angiogenic proteins by inflamed tenocytes. *Clinical Orthopaedics and Related Research* 473: 1624–1634. https://doi.org/10.1007/s11999-015-4179-z.
28. Heijnen, H., and P. van der Sluijs. 2015. Platelet secretory behaviour: As diverse as the granules … or not? *Journal of Thrombosis and Haemostasis* 13: 2141–2151. https://doi.org/10.1111/jth.13147.
29. Jonnalagadda, Deepa, Leighton T. Izu, and Sidney W. Whiteheart. 2012. Platelet secretion is kinetically heterogeneous in an agonist-responsive manner. *Blood* 120: 5209–5216. https://doi.org/10.1182/blood-2012-07-445080.
30. Kim, Joong Il, Hyun Cheol Bae, Hee Jung Park, Myung Chul Lee, and Hyuk Soo Han. 2020. Effect of Storage Conditions and Activation on Growth Factor Concentration in Platelet-Rich Plasma. *Journal of Orthopaedic Research* 38: 777–784. John Wiley & Sons, Ltd. https://doi.org/10.1002/jor.24520.
31. Barde, Y.A., D. Edgar, and H. Thoenen. 1982. Purification of a new neurotrophic factor from mammalian brain. *The EMBO Journal* 1: 549–553. https://doi.org/10.1002/j.1460-2075.1982.tb01207.x.
32. Bathina, Siresha, and Undurti N. Das. 2015. Brain-derived neurotrophic factor and its clinical implications. *Archives of Medical Science* 6: 1164–1178. https://doi.org/10.5114/aoms.2015.56342.
33. Lima Giacobbo, Bruno, Janine Doorduin, Hans C. Klein, Rudi A. J. O. Dierckx, Elke Bromberg, and Erik F. J. de Vries. 2019. Brain-derived neurotrophic factor in brain disorders: focus on neuroinflammation. *Molecular Neurobiology* 56: 3295–3312. Molecular Neurobiology. https://doi.org/10.1007/s12035-018-1283-6.
34. Kermani, Pouneh, and Barbara Hempstead. 2007. Brain-derived neurotrophic factor: A newly described mediator of angiogenesis. *Trends in Cardiovascular Medicine* 17: 140–143. https://doi.org/10.1016/j.tcm.2007.03.002.
35. Chen, Shang-Der., Wu. Chia-Lin, Wei-Chao. Hwang, and Ding-I. Yang. 2017. More insight into BDNF against neurodegeneration: Anti-apoptosis, anti-oxidation, and suppression of autophagy. *International Journal of Molecular Sciences* 18: 545. https://doi.org/10.3390/ijms18030545.
36. Ji, Xin Chao, Yuan Yuan Dang, Hong Yan Gao, Zhao Tao Wang, Mou Gao, Yi Yang, Hong Tian Zhang, and Ru Xiang Xu. 2015. Local injection of lenti–BDNF at the lesion site promotes M2 macrophage polarization and inhibits inflammatory response after spinal cord injury in mice. *Cellular and Molecular Neurobiology* 35, 881–890. Springer US. https://doi.org/10.1007/s10571-015-0182-x.
37. Zimmermann, Manfred. 1983. Ethical guidelines for investigations of experimental pain in conscious animals. *Pain* 16: 109–110. https://doi.org/10.1016/0304-3959(83)90201-4.
38. Lana, Jose Fabio, Santos Duarte, Joseph Purita, Christian Paulus, Stephany Cares Huber, Bruno Lima Rodrigues, Ana Amélia Rodrigues, Maria Helena Santana, et al. 2017. Contributions for classification of platelet rich plasma – proposal of a new classification: MARSPILL. *Regenerative Medicine* 12: 565–574. https://doi.org/10.2217/rme-2017-0042.
39. Amable, Paola Romina, Rosana Bizon Vieira. Carias, Marcus Vinicius Telles. Teixeira, Ítalo. da Cruz Pacheco, Ronaldo José Farias Corrêa. do Amaral, JoséMauro. Granjeiro, and Radovan Borojevic. 2013. Platelet-rich plasma preparation for regenerative medicine: Optimization and quantification of cytokines and growth factors. *Stem Cell Research and Therapy* 4: 1–13. https://doi.org/10.1186/scrt218.
40. Varga-Szabo, D., A. Braun, and Bernhard Nieswandt. 2009. Calcium signaling in platelets. *Journal of Thrombosis and Haemostasis* 7: 1057–1066. https://doi.org/10.1111/j.1538-7836.2009.03455.x.
41. Perez, Amanda G. M., Ana A. Rodrigues, Angela C. M. Luzo, José F. S. D. Lana, William D. Belangero, and Maria H. A. Santana. 2014. Fibrin network architectures in pure platelet-rich plasma as characterized by fiber radius and correlated with clotting time. *Journal of Materials Science: Materials in Medicine* 25: 1967–1977. https://doi.org/10.1007/s10856-014-5235-z.
42. Toda, Gotaro, Toshimasa Yamauchi, Takashi Kadowaki, and Kohjiro Ueki. 2021. Preparation and culture of bone marrow-derived macrophages from mice for functional analysis. *STAR Protocols* 2, 100246. Elsevier Inc. https://doi.org/10.1016/j.xpro.2020.100246.
43. Schmittgen, Thomas D., and Kenneth J. Livak. 2008. Analyzing real-time PCR data by the comparative CT method. *Nature Protocols* 3: 1101–1108. https://doi.org/10.1038/nprot.2008.73.
44. Guerrero, Ana T.G.., Waldiceu A. Verri, Thiago M. Cunha, Tarcilia A. Silva, Francisco A.C.. Rocha, Sérgio. H. Ferreira, Fernando Q. Cunha, and Carlos A. Parada. 2006. Hypernociception elicited by tibio-tarsal joint flexion in mice: A novel experimental arthritis model for pharmacological screening. *Pharmacology*

Biochemistry and Behavior 84: 244–251. https://doi.org/10.1016/j.pbb.2006.05.008.
45. Pritzker, Kenneth P.H.., S. Gay, S.A. Jimenez, K. Ostergaard, J.P. Pelletier, K. Revell, D. Salter, and W.B. van den Berg. 2006. Osteoarthritis cartilage histopathology: Grading and staging. *Osteoarthritis and Cartilage* 14: 13–29. https://doi.org/10.1016/j.joca.2005.07.014.
46. Pham, B., A. Cranney, M. Boers, A.C. Verhoeven, G. Wells, and P. Tugwell. 1999. Validity of area-under-the-curve analysis to summarize effect in rheumatoid arthritis clinical trials. *The Journal of rheumatology* 26: 712–716.
47. Kahan, Barry D., Maria Welsh, and Lynne P. Rutzky. 1995. Challenges in cyclosporine therapy: The role of therapeutic monitoring by area under the curve monitoring. *Therapeutic Drug Monitoring* 17: 621–624. https://doi.org/10.1097/00007691-199512000-00013.
48. Fujimura, Hironobu, C. Anthony Altar, Ruoyan Chen, Takashi Nakamura, Takeshi Nakahashi, Jun-ichi Ichi. Kambayashi, Bing Sun, and Narendra N. Tandon. 2002. Brain-derived neurotrophic factor is stored in human platelets and released by agonist stimulation. *Thrombosis and Haemostasis* 87: 728–734. https://doi.org/10.1055/s-0037-1613072.
49. Blanc, Le., Samuel Fleury Jessica, Imane Boukhatem, Jean Christophe Bélanger, Mélanie. Welman, and Marie Lordkipanidzé. 2020. Platelets selectively regulate the release of BDNF, but not that of its precursor protein, proBDNF. *Frontiers in Immunology* 11: 1–12. https://doi.org/10.3389/fimmu.2020.575607.
50. Martin, John F., and Günter. P. Wagner. 2019. The origin of platelets enabled the evolution of eutherian placentation. *Biology Letters* 15: 20190374. https://doi.org/10.1098/rsbl.2019.0374.
51. Plattner, Helmut, and Alexei Verkhratsky. 2016. Inseparable tandem: Evolution chooses ATP and Ca 2+ to control life, death and cellular signalling. *Philosophical Transactions of the Royal Society B: Biological Sciences* 371: 20150419. https://doi.org/10.1098/rstb.2015.0419.
52. Ren, Qiansheng, Holly Kalani Barber, Garland L. Crawford, Zubair A. Karim, Chunxia Zhao, Wangsun Choi, Cheng-Chun. Wang, Wanjin Hong, and Sidney W. Whiteheart. 2007. Endobrevin/VAMP-8 is the primary v-SNARE for the platelet release reaction. Edited by Sean Munro. *Molecular Biology of the Cell* 18: 24–33. https://doi.org/10.1091/mbc.e06-09-0785.
53. Escobar, Gisselle, Alejandro Escobar, Gabriel Ascui, Fabián I. Tempio, María C. Ortiz, Claudio A. Pérez, and Mercedes N. López. 2018. Pure platelet-rich plasma and supernatant of calcium-activated P-PRP induce different phenotypes of human macrophages. *Regenerative Medicine* 13: 427–441. https://doi.org/10.2217/rme-2017-0122.
54. Lam, Fong W., K. Vinod Vijayan, and Rolando E. Rumbaut. 2015. Platelets and their interactions with other immune cells. *Comprehensive Physiology* 5: 1265–1280. Wiley. https://doi.org/10.1002/cphy.c140074.
55. Chen, Yufei, Haoxuan Zhong, Yikai Zhao, Xinping Luo, and Wen Gao. 2020. Role of platelet biomarkers in inflammatory response. *Biomarker Research* 8: 28. Biomarker Research. https://doi.org/10.1186/s40364-020-00207-2.
56. Geraghty, Terese, Deborah R. Winter, Richard J. Miller, Rachel E. Miller, and Anne-Marie Malfait. 2021. Neuroimmune interactions and osteoarthritis pain: focus on macrophages. *PAIN Reports* 6: e892. Ovid Technologies (Wolters Kluwer Health). https://doi.org/10.1097/pr9.0000000000000892.
57. Sun, Yulong, Zhuo Zuo, and Yuanyuan Kuang. 2020. An emerging target in the battle against osteoarthritis: Macrophage polarization. *International Journal of Molecular Sciences* 21: 8513. https://doi.org/10.3390/ijms21228513.
58. Wang, Weiyun, Yaru Chu, Pengyuan Zhang, Zhuo Liang, Zhenlin Fan, Xueqiang Guo, Guangdong Zhou, and Wenjie Ren. 2023. Targeting macrophage polarization as a promising therapeutic strategy for the treatment of osteoarthritis. *International Immunopharmacology* 116: 109790. https://doi.org/10.1016/j.intimp.2023.109790.
59. Zhang, Wang, Yuntao Zhang, Yuxian He, Xiying Wang, and Qiang Fang. 2019. Lipopolysaccharide mediates time-dependent macrophage M1/M2 polarization through the Tim-3/Galectin-9 signalling pathway. *Experimental Cell Research* 376: 124–132. Elsevier Inc.. https://doi.org/10.1016/j.yexcr.2019.02.007.
60. Jiang, Guangyao, Sihao Li, Kang Yu, Bin He, Jianqiao Hong, Tengjing Xu, Jiahong Meng, et al. 2021. A 3D-printed PRP-GelMA hydrogel promotes osteochondral regeneration through M2 macrophage polarization in a rabbit model. *Acta Biomaterialia* 128: 150–162. Acta Materialia Inc. https://doi.org/10.1016/j.actbio.2021.04.010.
61. Kargarpour, Zahra, Jila Nasirzade, Layla Panahipour, Richard J. Miron, and Reinhard Gruber. 2021. Liquid PRF reduces the inflammatory response and osteoclastogenesis in murine macrophages. *Frontiers in Immunology* 12. Frontiers Media S.A. https://doi.org/10.3389/fimmu.2021.636427.
62. Nasirzade, Jila, Zahra Kargarpour, Sadegh Hasannia, Franz Josef Strauss, and Reinhard Gruber. 2020. Platelet-rich fibrin elicits an anti-inflammatory response in macrophages *in vitro*. *Journal of Periodontology* 91, 244–252. John Wiley and Sons Inc. https://doi.org/10.1002/JPER.19-0216.
63. Kowiański, Przemysław, Grażyna Lietzau, Ewelina Czuba, Monika Waśkow, Aleksandra Steliga, and Janusz Moryś. 2018. BDNF: A key factor with multipotent impact on brain signaling and synaptic plasticity. *Cellular and Molecular Neurobiology* 38: 579–593. https://doi.org/10.1007/s10571-017-0510-4.
64. Arranz, Alicia, Christina Doxaki, Eleni Vergadi, Martinez de la Torre, Katerina Vaporidi, Eleni D. Lagoudaki, Eleftheria Ieronymaki, et al. 2012. Akt1 and Akt2 protein kinases differentially contribute to macrophage polarization. *Proceedings of the National Academy of Sciences* 109: 9517–9522. https://doi.org/10.1073/pnas.1119038109.
65. Su, Yu-Wen., Xin-Fu. Zhou, Bruce K. Foster, Brian L. Grills, Xu. Jiake, and Cory J. Xian. 2018. Roles of neurotrophins in skeletal tissue formation and healing. *Journal of Cellular Physiology* 233: 2133–2145. https://doi.org/10.1002/jcp.25936.
66. Hutchison, Michele R. 2013. Mice with a conditional deletion of the neurotrophin receptor TrkB are dwarfed, and are similar to mice with a MAPK14 deletion. *Edited by Frank Beier. PLoS ONE* 8: e66206. https://doi.org/10.1371/journal.pone.0066206.
67. Hutchison, Michele R., Mary H. Bassett, and Perrin C. White. 2010. SCF, BDNF, and Gas6 are regulators of growth plate chondrocyte proliferation and differentiation. *Molecular Endocrinology* 24: 193–203. https://doi.org/10.1210/me.2009-0228.
68. Rihl, M., E. Kruithof, C. Barthel, F. De Keyser, E.M. Veys, H. Zeidler, D.T.Y. Yu, J.G. Kuipers, and D. Baeten. 2005. Involvement of neurotrophins and their receptors in spondyloarthritis synovitis: Relation to inflammation and response to treatment. *Annals of the Rheumatic Diseases* 64: 1542–1549. https://doi.org/10.1136/ard.2004.032599.
69. Iu, ElsieChitYu., and ChiBun Chan. 2022. Is Brain-derived neurotrophic factor a metabolic hormone in peripheral tissues? *Biology* 11: 1063. https://doi.org/10.3390/biology11071063.
70. Bryk, Marta, Jakub Chwastek, Jakub Mlost, Magdalena Kostrzewa, and Katarzyna Starowicz. 2021. Sodium monoiodoacetate dose-dependent changes in matrix metalloproteinases and inflammatory components as prognostic factors for the progression of osteoarthritis. *Frontiers in Pharmacology* 12: 1–16. https://doi.org/10.3389/fphar.2021.643605.
71. de Sousavalente, João. 2019. The pharmacology of pain associated with the monoiodoacetate model of osteoarthritis. *Frontiers*

in Pharmacology 10: 1–8. https://doi.org/10.3389/fphar.2019.00974.
72. Ogbonna, Andrea C., Anna K. Clark, and Marzia Malcangio. 2015. Development of monosodium acetate-induced osteoarthritis and inflammatory pain in ageing mice. *Age* 37. https://doi.org/10.1007/s11357-015-9792-y.
73. de Douglas Menezes , Kauê Franco Malange, Catarine Massucato Nishijima, Bruno Henrique de Melo Lima, Vinicius Cooper Capetini, Alexandre L. R. de Oliveira, Gabriel Forato Anhê, Claudia Herrera Tambeli, and Carlos Amilcar Parada. 2024. Intraarticular monomethyl fumarate as a perspective therapy for osteoarthritis by macrophage polarization. *Inflammopharmacology*. https://doi.org/10.1007/s10787-024-01443-w.
74. Moilanen, L.J., M. Hämäläinen, E. Nummenmaa, P. Ilmarinen, K. Vuolteenaho, R.M. Nieminen, L. Lehtimäki, and E. Moilanen. 2015. Monosodium iodoacetate-induced inflammation and joint pain are reduced in TRPA1 deficient mice - potential role of TRPA1 in osteoarthritis. *Osteoarthritis and Cartilage* 23: 2017–2026. https://doi.org/10.1016/j.joca.2015.09.008.
75. Korotkyi, O.H., A.A. Vovk, T.I. Galenova, T.B. Vovk, K.O. Dvorschenko, T.M. Falalyeyeva, and L.I. Ostapchenko. 2020. Cytokines profile in knee cartilage of rats during monoiodoacetateinduced osteoarthritis and administration of probiotic. *Biopolymers and Cell* 36: 23–35. https://doi.org/10.7124/bc.000A1E.
76. Kawarai, Yuya, Sumihisa Orita, Junichi Nakamura, Shuichi Miyamoto, Miyako Suzuki, Kazuhide Inage, Shigeo Hagiwara, et al. 2018. Changes in proinflammatory cytokines, neuropeptides, and microglia in an animal model of monosodium iodoacetate-induced hip osteoarthritis. *Journal of Orthopaedic Research* 36: 2978–2986. https://doi.org/10.1002/jor.24065.
77. Sakurai, Yusuke, Masahide Fujita, Shiori Kawasaki, Takao Sanaki, Takeshi Yoshioka, Kenichi Higashino, Soichi Tofukuji, et al. 2019. Contribution of synovial macrophages to rat advanced osteoarthritis pain resistant to cyclooxygenase inhibitors. *Pain* 160: 895–907. https://doi.org/10.1097/j.pain.0000000000001466.
78. Sousa-Valente, J., L. Calvo, V. Vacca, R. Simeoli, J.C. Arévalo, and M. Malcangio. 2018. Role of TrkA signalling and mast cells in the initiation of osteoarthritis pain in the monoiodoacetate model. *Osteoarthritis and Cartilage* 26: 84–94. https://doi.org/10.1016/j.joca.2017.08.006.
79. Muley, Milind M., Eugene Krustev, Allison R. Reid, and Jason J. McDougall. 2017. Prophylactic inhibition of neutrophil elastase prevents the development of chronic neuropathic pain in osteoarthritic mice. *Journal of Neuroinflammation* 14. BioMed Central Ltd. https://doi.org/10.1186/s12974-017-0944-0.
80. Guzman, Roberto E., Mark G. Evans, Susan Bove, Brandy Morenko, and Kenneth Kilgore. 2003. Mono-Iodoacetate-Induced Histologic Changes in Subchondral Bone and Articular Cartilage of Rat Femorotibial Joints: AN Animal Model of Osteoarthritis. *Toxicologic Pathology* 31: 619–624. https://doi.org/10.1080/01926230390241800.
81. Gao, Xin, Yaqing Ma, Guijiao Zhang, Fengyan Tang, Jingjing Zhang, Jichao Cao, and Chunhui Liu. 2020. Targeted elimination of intracellular reactive oxygen species using nanoparticle-like chitosan- superoxide dismutase conjugate for treatment of monoiodoacetate-induced osteoarthritis. *International Journal of Pharmaceutics* 590: 119947. Elsevier B.V.. https://doi.org/10.1016/j.ijpharm.2020.119947.
82. Moon, S.J., Y.J. Woo, J.H. Jeong, M.K. Park, H.J. Oh, J.S. Park, E.K. Kim, et al. 2012. Rebamipide attenuates pain severity and cartilage degeneration in a rat model of osteoarthritis by down-regulating oxidative damage and catabolic activity in chondrocytes. *Osteoarthritis and Cartilage* 20: 1426–1438. https://doi.org/10.1016/j.joca.2012.08.002.
83. Malange, Kaue Franco, Juliana M. Navia-Pelaez, Elayne Vieira Dias, Julia Borges Paes Lemes, Soo-Ho Choi, Gilson Goncalves Dos Santos, Tony L. Yaksh, and Maripat Corr. 2022. Macrophages and glial cells: Innate immune drivers of inflammatory arthritic pain perception from peripheral joints to the central nervous system. *Frontiers in Pain Research* 3. https://doi.org/10.3389/fpain.2022.1018800.
84. Aniss, Nadia Noble-Daoud., Asmaa Magdy Zaazaa, and Mohamed Rabie Abdall. Saleh. 2019. Anti-arthritic Effects of Platelets Rich Plasma and Hyaluronic Acid on Adjuvant-induced Arthritis in Rats. *International Journal of Pharmacology* 16: 33–46. https://doi.org/10.3923/ijp.2020.33.46.
85. Woodell-May, Jennifer, Andrea Matuska, Megan Oyster, Zachary Welch, Krista O'Shaughnessey, and Jacy Hoeppner. 2011. Autologous protein solution inhibits MMP-13 production by IL-1β and TNFα-stimulated human articular chondrocytes. *Journal of Orthopaedic Research* 29: 1320–1326. https://doi.org/10.1002/jor.21384.
86. Pitsillides, Andrew A., and Frank Beier. 2011. Cartilage biology in osteoarthritis—lessons from developmental biology. *Nature Reviews Rheumatology* 7: 654–663. https://doi.org/10.1038/nrrheum.2011.129.
87. Kita, Keisuke, Tohru Kimura, Norimasa Nakamura, Hideki Yoshikawa, and Toru Nakano. 2008. PI3K/Akt signaling as a key regulatory pathway for chondrocyte terminal differentiation. *Genes to Cells* 13: 839–850. https://doi.org/10.1111/j.1365-2443.2008.01209.x.
88. Xue, Fan, Zhenlei Zhao, Yanpei Gu, Jianxin Han, Keqiang Ye, and Ying Zhang. 2021. 7,8-dihydroxyflavone modulates bone formation and resorption and ameliorates ovariectomy-induced osteoporosis. *eLife* 10. eLife Sciences Publications Ltd. https://doi.org/10.7554/eLife.64872.
89. Lotz, Martin K., and Beatriz Caramés. 2011. Autophagy and cartilage homeostasis mechanisms in joint health, aging and OA. *Nature Reviews Rheumatology* 7: 579–587. https://doi.org/10.1038/nrrheum.2011.109.
90. Liao, Jiahe, Xinbo Yu, Jiaqi Chen, Zihua Wu, Qian He, Yan Zhang, Weijiang Song, Jing Luo, and Qingwen Tao. 2023. Knowledge mapping of autophagy in osteoarthritis from 2004 to 2022: A bibliometric analysis. *Frontiers in Immunology* 14. https://doi.org/10.3389/fimmu.2023.1063018.
91. Matsuzaki, Tokio, Oscar Alvarez-Garcia, Sho Mokuda, Keita Nagira, Merissa Olmer, Ramya Gamini, Kohei Miyata, et al. 2018. FoxO transcription factors modulate autophagy and proteoglycan 4 in cartilage homeostasis and osteoarthritis. *Science Translational Medicine* 10. https://doi.org/10.1126/scitranslmed.aan0746.
92. Wei, ChangWei, Yi Sun, Nan Chen, Song Chen, MeiHong Xiu, and XiangYang Zhang. 2020. Interaction of oxidative stress and BDNF on executive dysfunction in patients with chronic schizophrenia. *Psychoneuroendocrinology* 111: 104473. Elsevier. https://doi.org/10.1016/j.psyneuen.2019.104473.
93. He, Tongrong, and Zvonimir S. Katusic. 2012. Brain-derived neurotrophic factor increases expression of MnSOD in human circulating angiogenic cells. *Microvascular Research* 83: 366–371. Elsevier Inc. https://doi.org/10.1016/j.mvr.2012.01.001.
94. Zhu, Wawa, Gautam N. Bijur, Nathan A. Styles, and Xiaohua Li. 2004. Regulation of FOXO3a by brain-derived neurotrophic factor in differentiated human SH-SY5Y neuroblastoma cells. *Molecular Brain Research* 126: 45–56. https://doi.org/10.1016/j.molbrainres.2004.03.019.
95. Xu, Danfeng, Di Lian, Jing Wu, Ying Liu, Mingjie Zhu, Jiaming Sun, Dake He, and Ling Li. 2017. Brain-derived neurotrophic factor reduces inflammation and hippocampal apoptosis in experimental Streptococcus pneumoniae meningitis. *Journal*

of Neuroinflammation 14: 156. Journal of Neuroinflammation. https://doi.org/10.1186/s12974-017-0930-6.
96. Schaible, Hans-Georg. 2007. Nociceptors of the joint with particular reference to silent nociceptors. 15:18–27. https://doi.org/10.1159/000101965.
97. Grigg, Peter. 2001. Properties of sensory neurons innervating synovial joints. *Cells, Tissues, Organs* 169: 218–225. https://doi.org/10.1159/000047885.
98. McDougall, Jason J. 2006. Arthritis and pain. Neurogenic origin of joint pain. *Arthritis Research and Therapy* 8: 1–10. https://doi.org/10.1186/ar2069.
99. Schuelert, Niklas, and Jason J. McDougall. 2009. Grading of monosodium iodoacetate-induced osteoarthritis reveals a concentration-dependent sensitization of nociceptors in the knee joint of the rat. *Neuroscience Letters* 465: 184–188. https://doi.org/10.1016/j.neulet.2009.08.063.
100. Vieira, Willians Fernando, Kauê Franco. Malange, Silviane Fernandes, Gilson de Magalhães, Gonçalves dos Santos, Alexandre Leite Rodrigues, Maria de Oliveira, Alice da Cruz-Höfling, and Carlos Amilcar Parada. 2020. Gait analysis correlates mechanical hyperalgesia in a model of streptozotocin-induced diabetic neuropathy: A CatWalk dynamic motor function study. *Neuroscience Letters* 736: 135253. https://doi.org/10.1016/j.neulet.2020.135253.
101. Shepherd, Andrew J., and Durga P. Mohapatra. 2018. Pharmacological validation of voluntary gait and mechanical sensitivity assays associated with inflammatory and neuropathic pain in mice. *Neuropharmacology* 130: 18–29. Elsevier Ltd. https://doi.org/10.1016/j.neuropharm.2017.11.036.
102. Ferland, C. E., S. Laverty, F. Beaudry, and P. Vachon. 2011. Gait analysis and pain response of two rodent models of osteoarthritis. *Pharmacology Biochemistry and Behavior* 97: 603–610. Elsevier Inc. https://doi.org/10.1016/j.pbb.2010.11.003.
103. Çağlar, Ceyhun, Halil Kara, Okan Ateş, and Mahmut Uğurlu. 2021. Evaluation of Different Intraarticular Injection Therapies with Gait Analysis in a Rat Osteoarthritis Model. *Cartilage* 13: 1134S-1143S. SAGE Publications Inc. https://doi.org/10.1177/19476035211046042.
104. Ferreira-Gomes, Joana, Sara Adães, and José M. Castro-Lopes. 2008. Assessment of movement-evoked pain in osteoarthritis by the knee-bend and catwalk tests: A clinically relevant study. *Journal of Pain* 9: 945–954. https://doi.org/10.1016/j.jpain.2008.05.012.
105. Ferreira-Gomes, Joana, Sara Adães, Jana Sarkander, and José M. Castro-Lopes. 2010. Phenotypic alterations of neurons that innervate osteoarthritic joints in rats. *Arthritis Care and Research* 62: 3677–3685. https://doi.org/10.1002/art.27713.
106. Ghilardi, Joseph R., Katie T. Freeman, Juan M. Jimenez-Andrade, Kathleen A. Coughlin, Magdalena J. Kaczmarska, Gabriela Castaneda-Corral, Aaron P. Bloom, Michael A. Kuskowski, and Patrick W. Mantyh. 2012. Neuroplasticity of sensory and sympathetic nerve fibers in a mouse model of a painful arthritic joint. *Arthritis & Rheumatism* 64: 2223–2232. https://doi.org/10.1002/art.34385.
107. Kral, Julia Barbara, Waltraud Cornelia Schrottmaier, Manuel Salzmann, and Alice Assinger. 2016. Platelet interaction with innate immune cells. *Transfusion Medicine and Hemotherapy* 43: 78–88. https://doi.org/10.1159/000444807.
108. Yuan, Zimu, Decheng Jiang, Mengzhu Yang, Jie Tao, Hu. Xin, Xiao Yang, and Yi. Zeng. 2024. Emerging roles of macrophage polarization in osteoarthritis: Mechanisms and therapeutic strategies. *Orthopaedic Surgery* 16: 532–550. https://doi.org/10.1111/os.13993.
109. Tsujino, Hiroaki, Eiji Kondo, Tetsuo Fukuoka, Yi Dai, Atsushi Tokunaga, Kenji Miki, Kazuo Yonenobu, Takahiro Ochi, and Koichi Noguchi. 2000. Activating Transcription Factor 3 (ATF3) Induction by axotomy in sensory and motoneurons: A novel neuronal marker of nerve injury. 182: 170–182. https://doi.org/10.1006/mcne.1999.0814.
110. Bráz, João. M., and Allan I. Basbaum. 2010. Differential ATF3 expression in dorsal root ganglion neurons reveals the profile of primary afferents engaged by diverse noxious chemical stimuli. *Pain* 150: 290–301. https://doi.org/10.1016/j.pain.2010.05.005.
111. Sant'Anna, Morena B., Ricardo Kusuda, Tiago A. Bozzo, Gabriel S. Bassi, Jose C. Alves-Filho, Fernando Q. Cunha, Sergio H. Ferreira, Guilherme R. Souza, and Thiago M. Cunha. 2016. Medial plantar nerve ligation as a novel model of neuropathic pain in mice: Pharmacological and molecular characterization. *Scientific Reports* 6: 1–13. Nature Publishing Group. https://doi.org/10.1038/srep26955.
112. Griffith, Oliver W., Arun R. Chavan, Stella Protopapas, Jamie Maziarz, Roberto Romero, and Gunter P. Wagner. 2017. Embryo implantation evolved from an ancestral inflammatory attachment reaction. *Proceedings of the National Academy of Sciences* 114: E6566–E6575. https://doi.org/10.1073/pnas.1701129114.
113. Lana, José Fábio., Stephany Cares Huber, Joseph Purita, Claudia H. Tambeli, Gabriel Silva Santos, Christian Paulus, and Joyce M. Annichino-Bizzacchi. 2019. Leukocyte-rich PRP versus leukocyte-poor PRP - The role of monocyte/macrophage function in the healing cascade. *Journal of Clinical Orthopaedics and Trauma* 10: S7–S12. https://doi.org/10.1016/j.jcot.2019.05.008.
114. Liang, Jiedong, Gui Deng, and He Huang. 2018. The activation of BDNF reduced inflammation in a spinal cord injury model by TrkB/p38 MAPK signaling. *Experimental and Therapeutic Medicine* 1688–1696. https://doi.org/10.3892/etm.2018.7109.
115. Asami, Toshio, Takuya Ito, Hidefumi Fukumitsu, Hiroshi Nomoto, Yoshiko Furukawa, and Shoei Furukawa. 2006. Autocrine activation of cultured macrophages by brain-derived neurotrophic factor. *Biochemical and Biophysical Research Communications* 344: 941–947. https://doi.org/10.1016/j.bbrc.2006.03.228.
116. Barouch, Rina, Elena Appel, Gila Kazimirsky, and Chaya Brodie. 2001. Macrophages express neurotrophins and neurotrophin receptors. *Journal of Neuroimmunology* 112: 72–77. https://doi.org/10.1016/s0165-5728(00)00408-2.
117. Vun, James, Neelam Iqbal, Elena Jones, and Payal Ganguly. 2023. Anti-Aging Potential of Platelet Rich Plasma (PRP): Evidence from Osteoarthritis (OA) and applications in senescence and inflammaging. *Bioengineering* 10: 987. https://doi.org/10.3390/bioengineering10080987.
118. Yuan, Zimu, Decheng Jiang, Mengzhu Yang, Jie Tao, Hu. Xin, Xiao Yang, and Yi. Zeng. 2024. Emerging roles of macrophage polarization in osteoarthritis: Mechanisms and therapeutic strategies. *Orthopaedic Surgery* 9999: 9999. https://doi.org/10.1111/os.13993.
119. Nishio, Hirofumi, Yoshitomo Saita, Yohei Kobayashi, Tomoiku Takaku, Shin Fukusato, Sayuri Uchino, Takanori Wakayama, Hiroshi Ikeda, and Kazuo Kaneko. 2020. Platelet-rich plasma promotes recruitment of macrophages in the process of tendon healing. *Regenerative Therapy* 14: 262–270. Elsevier Ltd. https://doi.org/10.1016/j.reth.2020.03.009.
120. Swearingen, C.A., M.G. Chambers, C. Lin, J. Marimuthu, C.J. Rito, Q.L. Carter, J. Dotzlaf, et al. 2010. A short-term pharmacodynamic model for monitoring aggrecanase activity: Injection of monosodium iodoacetate (MIA) in rats and assessment of aggrecan neoepitope release in synovial fluid using novel ELISAs. *Osteoarthritis and Cartilage* 18: 1159–1166. https://doi.org/10.1016/j.joca.2010.02.019.
121. Mushenkova, Nataliya V., Nikita G. Nikiforov, Nikolay K. Shakhpazyan, Varvara A. Orekhova, Nikolay K. Sadykhov, and Alexander N. Orekhov. 2022. Phenotype diversity of macrophages in osteoarthritis: Implications for development of macrophage

modulating therapies. *International Journal of Molecular Sciences* 23: 8381. https://doi.org/10.3390/ijms23158381.
122. Sheikh, Ashfaq M., Mazhar Malik, Guang Wen, Abha Chauhan, Ved Chauhan, Cheng-Xin. Gong, Fei Liu, William T. Brown, and Xiaohong Li. 2010. BDNF-Akt-Bcl2 antiapoptotic signaling pathway is compromised in the brain of autistic subjects. *Journal of Neuroscience Research* 88: 2641–2647. https://doi.org/10.1002/jnr.22416.
123. Pérez-Navarro, Esther, Núria. Gavaldà, Elena Gratacòs, and Jordi Alberch. 2005. Brain-derived neurotrophic factor prevents changes in Bcl-2 family members and caspase-3 activation induced by excitotoxicity in the striatum. *Journal of Neurochemistry* 92: 678–691. https://doi.org/10.1111/j.1471-4159.2004.02904.x.
124. Ferreira-Gomes, Joana, Sara Adães, Jana Sarkander, and José M. Castro-Lopes. 2010. Phenotypic alterations of neurons that innervate osteoarthritic joints in rats. *Arthritis and Rheumatism* 62: 3677–3685. https://doi.org/10.1002/art.27713.
125. Ivanavicius, Stefan P., Adrian D. Ball, Chris G. Heapy, F Russell Westwood, Fraser Murray, and Simon J. Read. 2007. Structural pathology in a rodent model of osteoarthritis is associated with neuropathic pain: Increased expression of ATF-3 and pharmacological characterisation. *Pain* 128: 272–282. https://doi.org/10.1016/j.pain.2006.12.022.
126. Ferreira-Gomes, Joana, Sara Adães, Raquel M. Sousa, Marcelo Mendonça, and José M. Castro-Lopes. 2012. Dose-dependent expression of neuronal injury markers during experimental osteoarthritis induced by monoiodoacetate in the rat. *Molecular Pain* 8: 1–12. https://doi.org/10.1186/1744-8069-8-50.
127. Tao, Ranyang, Bobin Mi, Hu. Yiqiang, Sien Lin, Yuan Xiong, Lu. Xuan, Adriana C. Panayi, Gang Li, and Guohui Liu. 2023. Hallmarks of peripheral nerve function in bone regeneration. *Bone Research* 11: 6. https://doi.org/10.1038/s41413-022-00240-x.
128. Drissi, Ichrak, William Aidan Woods, and Christopher Geoffrey Woods. 2020. Understanding the genetic basis of congenital insensitivity to pain. *British Medical Bulletin* 133: 65–78. https://doi.org/10.1093/bmb/ldaa003.
129. Minde, Jan, Olle Svensson, Monica Holmberg, Göran. Solders, and Göran. Toolanen. 2006. Orthopedic aspects of familial insensitivity to pain due to a novel nerve growth factor beta mutation. *Acta Orthopaedica* 77: 198–202. https://doi.org/10.1080/17453670610045911.
130. Malfait, Anne Marie, Rachel E. Miller, and Joel A. Block. 2020. Targeting neurotrophic factors: Novel approaches to musculoskeletal pain. *Pharmacology and Therapeutics*. Elsevier Inc. https://doi.org/10.1016/j.pharmthera.2020.107553.
131. Miller, Rachel E., Joel A. Block, and Anne-Marie. Malfait. 2017. Nerve growth factor blockade for the management of osteoarthritis pain: What can we learn from clinical trials and preclinical models? *Current Opinion in Rheumatology* 29: 110–118. https://doi.org/10.1097/BOR.0000000000000354.
132. Chang, Yi., Ta Liang Chen, Wu. Gong Jhe, George Hsiao, Ming Yi Shen, Kuan Hung Lin, Duen Suey Chou, Chien Huang Lin, and Joen Rong Sheu. 2004. Mechanisms involved in the antiplatelet activity of ketamine in human platelets. *Journal of Biomedical Science* 11: 764–772. https://doi.org/10.1159/000081823.
133. Nakagawa, Takefumi, Hideo Hirakata, Masami Sato, Kumi Nakamura, Yoshio Hatano, Takashi Nakamura, and Kazuhiko Fukuda. 2002. Ketamine Suppresses Platelet Aggregation Possibly by Suppressed Inositol Triphosphate Formation and Subsequent Suppression of Cytosolic Calcium Increase. *Anesthesiology* 96: 1147–1152. https://doi.org/10.1097/00000542-200205000-00018.

This work was derived from the doctoral thesis of Kaue Franco Malange.